Halide-Promoted Carbonylation of the Imido Ligand in $Os_3(\mu_3\text{-NPh})(CO)_{10}$

David L. Ramage and Gregory L. Geoffroy*

Department of Chemistry, The Pennsylvania State University, University Park, Pennsylvania 16802

Arnold L. Rheingold and Brian S. Haggerty

Department of Chemistry, University of Delaware, Newark, Delaware 19716

Received September 26, 1991

The imido cluster $Os_3(\mu_3\text{-NPh})(CO)_{10}$ has been found to react with halides to give the isomeric clusters $[PPN][Os_3(\mu_3\text{-NPh})(\mu_2\text{-X})(CO)_9]$ (**7**) and $[PPN][Os_3(\mu_3\text{-NPh})(X)(CO)_9]$ (**8**), which have bridging and terminal halide ligands, respectively, with the ratio of the isomers dependent upon the halide used. For chloride, the major isomer is **7**, which has been crystallographically shown to have two Os–Os bonds and the chloride ligand bridging two nonbonded Os atoms. For iodide, the major isomer is **8**, which has three Os–Os bonds and a terminal iodide ligand. Both isomers are present in nearly equal amounts when X = Br. The parent imido cluster $Os_3(\mu_3\text{-NPh})(CO)_{10}$ is inert to carbonylation, but when the isomeric halide-substituted clusters are placed under 1 atm of CO at 22 °C, slow carbonylation occurs to form the two new clusters $[Os_3(\eta^2\text{-}\mu_3\text{-PhNCO})(\mu_2\text{-X})(CO)_9]^-$ (**12**) and $[Os_3(\eta^2\text{-}\mu_2\text{-PhNCO})(\mu_2\text{-X})(CO)_{10}]^-$ (**13**), which possess bridging PhNCO ligands resulting from the insertion of CO into the Os–N bond. When left under CO, these clusters further carbonylate to release free PhN=C=O and form the known compounds $[Os_3(X)(CO)_{11}]^-$. The oxygen atom of the $\eta^2\text{-}\mu_2$-PhNCO ligand in **13** can be protonated and alkylated with CF_3CO_2H and $CF_3SO_3CH_3$, respectively, to give the clusters $Os_3(\eta^2\text{-}\mu_2\text{-PhNCOR})(\mu_2\text{-X})(CO)_{10}$ (R = H, Me; X = Cl, I), of which the R = Me, X = I derivative has been crystallographically characterized.

Introduction

Halides have been shown to markedly promote the $Ru_3(CO)_{12}$-catalyzed carbonylation of nitroaromatics in the presence of methanol to form carbamates (eq 1).[1] Insight

$$PhNO_2 + MeOH + CO \xrightarrow[165°C,\ 82\ atm,\ 5\ h]{Ru_3(CO)_{12}} PhNH\text{-}\overset{\overset{O}{\|}}{C}\text{-}OMe + Ph\text{-}NH_2 \qquad (1)$$

toluene

promoter	conversion	carbamate yield	aniline yield
none	36%	22%	34%
$[Et_4N]^+Cl^-$	100%	93%	7%
$[Et_4N]^+I^-$	46%	64%	28%

into the possible role of the halide promoters in this catalytic system was earlier gained in these laboratories by the demonstration that halides promote the formation of imido ligands on triruthenium clusters from nitroso reagents and also promote the subsequent carbonylation of the imido ligands to form isocyanates.[2] It was demonstrated in that work that the halide-substituted clusters **2a–c** (Scheme I) rapidly formed from the reaction of PhNO with $Ru_3(CO)_{12}$ in the presence of halides and also that these clusters formed from the direct reaction of $Ru_3(\mu_3\text{-NPh})(CO)_{10}$ (**1**) with halides. Clusters **2a–c** were in turn found to react with CO to form PhN=C=O under conditions far milder than required to induce the carbonylation of the imido ligand of **1** in the absence of halides.[3] No intermediates were detected in the carbonylation of **2a–c**, but it was proposed that this transformation occurred by the sequence of events shown in Scheme II.[2a] The terminal halide ligand of **2** was proposed to displace

Scheme I

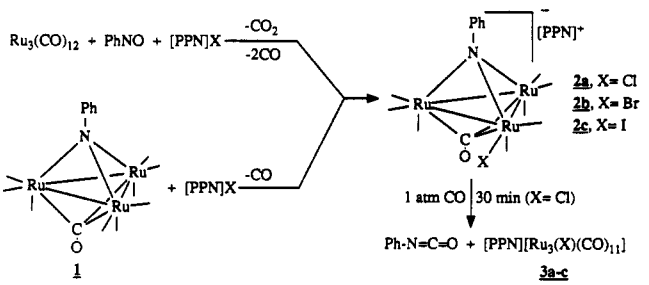

Scheme II

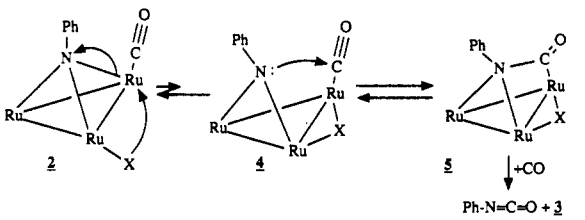

one of the Ru–NPh bonds by moving to a μ_2 bridging position to yield intermediate **4** with a μ_2-imido ligand. The nitrogen atom of this ligand could then add to an adjacent carbonyl ligand to produce cluster **5**, which possesses a coordinated isocyanate ligand which could then be displaced by CO to yield free phenyl isocyanate and cluster **3**.

In the work described herein, we set out to test the mechanistic suggestions of Scheme II by using osmium imido clusters in place of the ruthenium species. Triosmium clusters are known to be substantially less reactive than their triruthenium analogues, and hence we expected intermediates analogous to **4** and **5** to be substantially more stable with this metal than with ruthenium. As described below, we have indeed found that the imido cluster $Os_3(\mu_3\text{-NPh})(CO)_{10}$ (**6**) reacts with halides to form the isomeric halide-substituted clusters $[Os_3(\mu_3\text{-NPh})(X)(CO)_9]^-$ and $[Os_3(\mu_3\text{-NPh})(\mu_2\text{-X})(CO)_9]^-$ and that these species undergo subsequent carbonylation to yield clusters possessing co-

(1) Cenini, S.; Cortti, C.; Pizzotti, M.; Porta, F. *J. Org. Chem.* **1988**, *53*, 1243.

(2) (a) Han, S. H.; Geoffroy, G. L.; Rheingold, A. L. *Inorg. Chem.* **1987**, *26*, 3426. (b) Han, S. H.; Macklin, P. D.; Nguyen, S. T.; Geoffroy, G. L. *Organometallics* **1989**, *8*, 2127.

(3) (a) Smieja, J. A.; Gozum, J. E.; Gladfelter, W. L. *Organometallics* **1987**, *6*, 1311. (b) Basu, A.; Bhaduri, S.; Khwaja, H. *J. Organomet. Chem.* **1987**, *319*, C28.

0276-7333/92/2311-1242$03.00/0

Table I. Crystal Data for [PPN][$Os_3(\mu_3$-NPh)(μ_2-Cl)$(CO)_9$] (7a), $Os_3(\mu_2$-PhNH)(μ_2-Cl)$(CO)_{10}$ (10a), $Os_3(\mu_2$-HNPh)(μ_2-Cl)$(CO)_{10}$ (11a), and $Os_3(\eta^2\text{-}\mu_2\text{-}PhNCOCH_3)(\mu_2\text{-}I)(CO)_{10}$ (17c)

	7a	10a	11a	17c
	(a) Crystal Parameters			
formula	$C_{51}H_{35}ClN_2O_9Os_3P_2$	$C_{16}H_6ClNO_{10}Os_3$	$C_{16}H_6ClNO_{10}Os_3$	$C_{18}H_8INO_{11}Os_3$
fw	1487.85	977.27	977.27	1167.83
cryst system	monoclinic	monoclinic	orthorhombic	monoclinic
space group	$P2_1/c$	$C2/c$	$Pccn$	$C2/c$
a, Å	19.685 (3)	16.286 (3)	26.423 (5)	22.110 (11)
b, Å	15.258 (2)	17.059 (3)	13.069 (2)	16.151 (6)
c, Å	18.650 (3)	17.422 (4)	12.446 (2)	17.085 (8)
β, deg	117.744 (13)	118.51 (2)		114.03 (3)
V, Å^3	4957.8 (15)	4253.0 (17)	4297.8 (15)	5572 (4)
Z	4	8	8	8
cryst dimens, mm	0.19 × 0.28 × 0.42	0.36 × 0.41 × 0.42	0.29 × 0.30 × 0.42	0.38 × 0.41 × 0.52
cryst color	burnt-orange	yellow	yellow	golden-yellow
D(calc), g cm^3	1.993	3.052	3.020	2.784
μ(Mo Kα), cm^{-1}	78.55	90.44	179.00	148.10
temp, K	297	297	297	297
T(max)/T(min)	1.820	5.500	6.173	3.800
	(b) Data Collection			
diffractometer	Nicolet R3m			
monochromator	graphite			
radiation	Mo Kα (λ = 0.71073 Å)			
2θ scan range, deg	4–48	4–50	4–52	4–42
data collcd (h,k,l)	±23,+18,+22	±20,+21,+21	+33,+17,+16	±23,+17,+18
no. of rflns collcd	8297	3880	4740	3952
no. of indpt rflns	7706	3621	4230	3629
no. of indpt obsvd rflns [$F_o \geq n\sigma(F_o)$ (n = 5)]	5080	2698	2699	2461
std rflns	3 std/197 rflns	3 std/197 rflns	3 std/197 rflns	3 std/197 rflns
var in stds	~5	~4	~3	<2
	(c) Refinement			
$R(F)$, %	3.98	6.31	5.53	6.14
$R(F_w)$, %	3.90	6.52	5.87	6.52
Δ/σ(max)	0.062	0.054	0.002	0.012
$\Delta(\rho)$, e Å^{-3}	0.982	3.205	3.517	1.625
N_o/N_v	9.6	9.5	10.8	8.0
GOF	1.013	1.427	1.215	1.178

ordinated isocyanate ligands.

Results

Reaction of $Os_3(\mu_3$-NPh)$(CO)_{10}$ with Halides. The cluster $Os_3(\mu_3$-NPh)$(CO)_{10}$ (**6**)[4] was found to slowly react with [PPN]Cl to form the salt [PPN][$Os_3(\mu_3$-NPh)(μ_2-Cl)$(CO)_9$] (**7a**) (eq 2), which was isolated as an yellow-or-

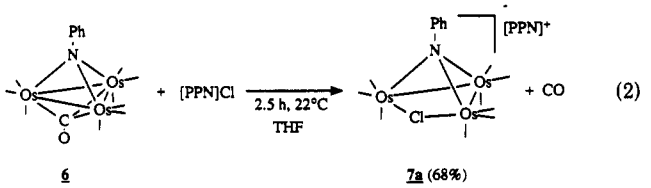

6 **7a** (68%)

ange microcrystalline powder and has been crystallographically characterized. The spectroscopic data for **7a** are summarized in the Experimental Section and are fully consistent with the determined structure. An ORTEP drawing of this anion is shown in Figure 1, and pertinent crystallographic data are given in Tables I–III. The cluster possesses two Os–Os bonds of lengths 2.748 (1) and 2.740 (1) Å and a nonbonded Os(1)···Os(2) separation of 3.359 (1) Å. The chloride ligand symmetrically bridges the nonbonded Os atoms with Os(1)–Cl and Os(2)–Cl bond lengths of 2.481 (4) and 2.483 (3) Å, respectively, which compare to the 2.466 (7) Å average Os–Cl bond length in $Os_3(\mu_2\text{-}Cl)_2(CO)_{10}$.[5] The Os–Cl–Os bond angle of 85.1 (1)° also compares well to the average Os–Cl–Os bond angle of 82.4 (5)° in $Os_3(\mu_2\text{-}Cl)_2(CO)_{10}$.[5] The phenylimido ligand

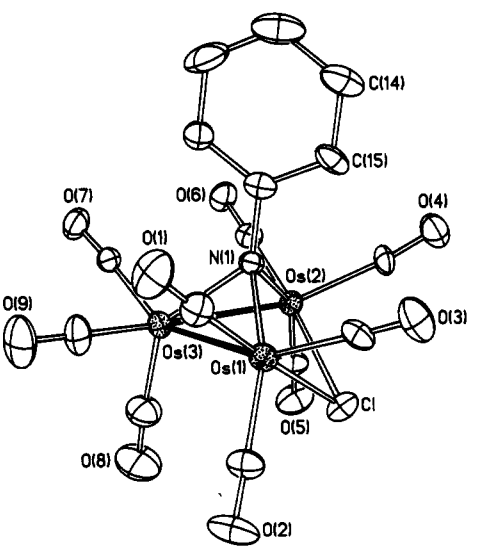

Figure 1. ORTEP drawing of the anion of [PPN][$Os_3(\mu_3$-NPh)(μ_2-Cl)$(CO)_9$] (**7a**). Thermal ellipsoids are drawn at the 35% probability level.

caps one face of the Os triangle, and the three Os–N bond lengths average 2.108 [13] Å.[6] The structure of **7a** is similar to that previously established for $Fe_3(\mu_3$-$SBu^t)(\mu_2$-Cl)$(CO)_9$[7] but differs from that of the crystallo-

(4) Smieja, J. A.; Gladfelter, W. L. *Inorg. Chem.* **1986**, *25*, 2667.
(5) Einstein, F. W. B.; Jones, T.; Tyers, K. G. *Acta Crystallogr.* **1982**, *B38*, 1272.

(6) Error estimates in brackets are exterior estimates of the precision of the average value. This is given by $[\sum_n(\bar{d} - d)^2/(n^2 - n)]^{1/2}$, where d is the bond distance or angle.
(7) (a) King, R. B.; Treichel, P. M.; Stone, F. G. A. *J. Am. Chem. Soc.* **1961**, *83*, 3600. (b) Winter, A.; Zsolnai, L.; Huttner, G. *J. Organomet. Chem.* **1982**, *232*, 47.

Table II. Atomic Coordinates (×10⁴) and Isotropic Thermal Parameters (Å² × 10³) for [PPN][Os₃(μ₃-NPh)(μ₂-Cl)(CO)₉] (7a)

	x	y	z	U[a]
Os(1)	1646.5 (3)	7983.8 (3)	2756.5 (3)	37.1 (2)
Os(2)	2616.2 (3)	6651.2 (3)	2122.2 (3)	32.4 (2)
Os(3)	2832.7 (3)	6868.7 (3)	3672.9 (3)	36.2 (2)
Cl	2291 (2)	8234 (2)	1905 (2)	49 (2)
P(1)	3231 (2)	1085 (2)	1495 (2)	38 (1)
P(2)	2684 (2)	2770 (2)	560 (2)	35 (1)
O(1)	866 (6)	7511 (7)	3772 (6)	80 (6)
O(2)	2056 (6)	9823 (6)	3456 (7)	86 (6)
O(3)	89 (5)	8441 (6)	1350 (5)	69 (5)
O(4)	1635 (5)	6188 (7)	332 (5)	70 (5)
O(5)	4122 (5)	7115 (6)	2124 (6)	72 (5)
O(6)	3124 (5)	4781 (5)	2537 (5)	52 (4)
O(7)	3477 (5)	5073 (5)	4335 (5)	58 (5)
O(8)	4301 (7)	7889 (9)	4170 (8)	129 (8)
O(9)	2650 (7)	7248 (7)	5172 (6)	90 (6)
N(1)	1820 (5)	6654 (6)	2600 (5)	33 (4)
N(2)	3203 (5)	2046 (6)	1157 (6)	45 (5)
C(1)	1169 (7)	7714 (8)	3389 (7)	49 (6)
C(2)	1895 (7)	9139 (8)	3188 (8)	49 (6)
C(3)	682 (7)	8271 (8)	1866 (7)	47 (6)
C(4)	1985 (6)	6410 (8)	979 (6)	41 (5)
C(5)	3551 (7)	6921 (8)	2121 (8)	45 (6)
C(6)	2908 (7)	5509 (8)	2370 (7)	43 (6)
C(7)	3236 (7)	5735 (7)	4057 (7)	43 (6)
C(8)	3736 (7)	7501 (10)	4009 (9)	70 (8)
C(9)	2705 (8)	7113 (9)	4576 (7)	59 (7)
C(11)	1269 (5)	5367 (6)	2915 (4)	56 (7)
C(12)	661	4783	2705	89 (11)
C(13)	5	4861	1958	82 (10)
C(14)	−43	5524	1422	67 (8)
C(15)	566	6109	1632	51 (6)
C(16)	1221	6030	2378	39 (6)
C(21)	1875 (4)	547 (5)	1456 (4)	49 (7)
C(22)	1163	129	1099	57 (7)
C(23)	920	−317	368	63 (7)
C(24)	1390	−345	−8	71 (8)
C(25)	2101	74	349	44 (6)
C(26)	2344	520	1080	35 (5)
C(31)	3883 (4)	−482 (5)	1330 (5)	51 (6)
C(32)	4437	−957	1226	60 (7)
C(33)	5007	−518	1123	65 (8)
C(34)	5023	396	1123	70 (8)
C(35)	4469	871	1226	54 (6)
C(36)	3899	432	1329	37 (5)
C(41)	3872 (5)	1898 (4)	2997 (5)	62 (7)
C(42)	4182	1908	3839	74 (8)
C(43)	4199	1140	4253	69 (8)
C(44)	3907	363	3825	61 (7)
C(45)	3597	353	2983	49 (6)
C(46)	3579	1121	2569	44 (6)
C(51)	2968 (4)	4500 (5)	323 (4)	53 (7)
C(52)	3425	5249	498	71 (10)
C(53)	4179	5231	1119	65 (8)
C(54)	4477	4464	1564	90 (9)
C(55)	4020	3716	1388	60 (7)
C(56)	3265	3734	768	38 (5)
C(61)	1765 (4)	3833 (4)	962 (4)	46 (6)
C(62)	1093	4035	1004	57 (7)
C(63)	487	3436	721	52 (7)
C(64)	554	2637	396	51 (6)
C(65)	1226	2435	355	48 (6)
C(66)	1831	3033	637	33 (5)
C(71)	1716 (5)	2947 (5)	−1073 (5)	70 (7)
C(72)	1490	2801	−1891	94 (10)
C(73)	1901	2217	−2118	96 (11)
C(74)	2538	1780	−1527	82 (11)
C(75)	2764	1927	−708	60 (8)
C(76)	2353	2510	−481	41 (6)

[a] Equivalent isotropic U defined as one-third of the trace of the orthogonalized U_{ij} tensor.

graphically characterized $[Ru_3(\mu_3\text{-NPh})(I)(CO)_9]^-$ (**2a**) (see Scheme I), which has a terminal iodide ligand and three Ru–Ru bonds,[2a] and $[Ru_3(\mu_3\text{-NPh})(Cl)(CO)_9]^-$ (**2c**), for

Table III. Selected Bond Distances and Bond Angles for [PPN][Os₃(μ₃-NPh)(μ₂-Cl)(CO)₉] (7a)

(a) Bond Distances (Å)

Os(1)–Os(3)	2.748 (1)	Os(1)–N(1)	2.100 (9)
Os(2)–Os(3)	2.740 (1)	Os(2)–N(1)	2.134 (11)
Os(1)···Os(2)	3.359 (1)	Os(3)–N(1)	2.091 (7)
Os(1)–Cl	2.481 (4)	N(1)–C(16)	1.418 (12)
Os(2)–Cl	2.483 (3)		

(b) Bond Angles (deg)

Os(3)–Os(1)–N(1)	48.9 (2)	Os(2)–Os(3)–N(1)	50.3 (3)
Os(3)–Os(1)–Cl	87.3 (1)	Os(1)–Cl–Os(2)	85.1 (1)
Cl–Os(1)–N(1)	84.0 (3)	Os(1)–N(1)–Os(2)	105.0 (4)
Os(3)–Os(2)–Cl	87.5 (1)	Os(1)–N(1)–Os(3)	82.0 (3)
Os(3)–Os(2)–N(1)	48.9 (2)	Os(2)–N(1)–Os(3)	80.9 (3)
Cl–Os(2)–N(1)	83.3 (2)	Os(1)–N(1)–C(16)	121.5 (7)
Os(1)–Os(3)–Os(2)	75.5 (1)	Os(2)–N(1)–C(16)	123.2 (7)
Os(1)–Os(3)–N(1)	49.2 (2)	Os(3)–N(1)–C(16)	132.6 (6)

which IR[2a] and ^{13}C NMR[8] spectroscopic data indicate a structure similar to **2a**.

The imido cluster $Os_3(\mu_3\text{-NPh})(CO)_{10}$ also reacts with [PPN]I to yield the salt $[PPN][Os_3(\mu_3\text{-NPh})(I)(CO)_9]$. This stoichiometry was indicated by elemental analysis and mass spectrometry (see Experimental Section), although its IR and ^{13}C NMR spectra indicate it to be a ~9:1 mixture of two compounds. The IR spectrum of the product differs from that of **7a** described above but is similar in band position and intensity to that of $[Ru_3(\mu_3\text{-NPh})(I)(CO)_9]^-$ (**2c**), which has been crystallographically demonstrated to have the structure drawn in Scheme I.[2a] A similar structure is thus proposed for the major product (**8c**) of the reaction of $Os_3(\mu_3\text{-NPh})(CO)_{10}$ with [PPN]I (eq 3). Particularly indicative of this structure

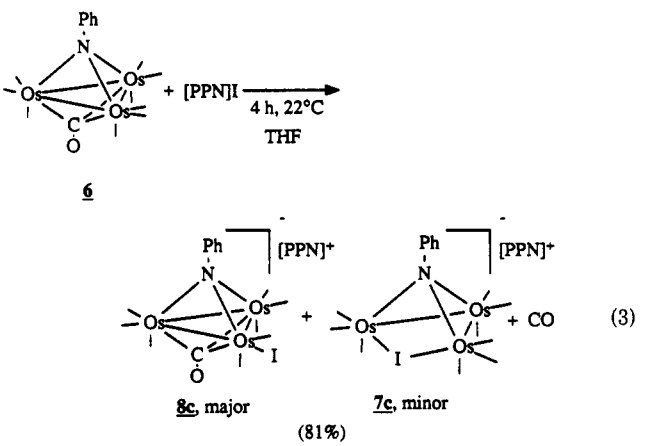

is the presence of a ν_{CO} band at 1657 cm^{-1} assigned to the face-bridging CO ligand, which compares to the corresponding band of **2c** at 1707 cm^{-1}. This 50-cm^{-1} difference corresponds exactly to the 50-cm^{-1} difference in the bands due to the μ_3-CO ligands in the parent compounds **1** (1724 cm^{-1}) and **6** (1674 cm^{-1}). The ^{13}C NMR spectrum of the product mixture recorded at −73 °C is also consistent with the structure proposed for the major product. It is similar to that of $[PPN][Ru_3(\mu_3\text{-NPh})(Cl)(CO)_9]$[8] in showing nine resonances integrating to one carbon each and assigned to the nine inequivalent CO ligands (see Experimental Section). Eight of these are in the terminal carbonyl region between δ 173–185. The ninth resonance at δ 234.4 is assigned to the μ_3-CO ligand. Also observed in the ^{13}C NMR spectrum of this product mixture were several weak

(8) **2a**: ^{13}C NMR (THF-d_8, −63 °C) δ 255.9 (s, 1 C, μ_3-CO), 203.0 (s, 1 C, Ru–CO), 201.3 (s, 1 C, Ru–CO), 201.1 (s, 1 C, Ru–CO), 199.0 (s, 1 C, Ru–CO), 198.9 (s, 1 C, Ru–CO), 198.8 (s, 1 C, Ru–CO), 194.1 (s, 1 C, Ru–CO), 193.5 (s, 1 C, Ru–CO), 165.8 (t, $^2J_{CH}$ = 4.1 Hz, 1 C, PhN *ipso*-C), 136–121 (PhN and $[PPN]^+$ carbons).

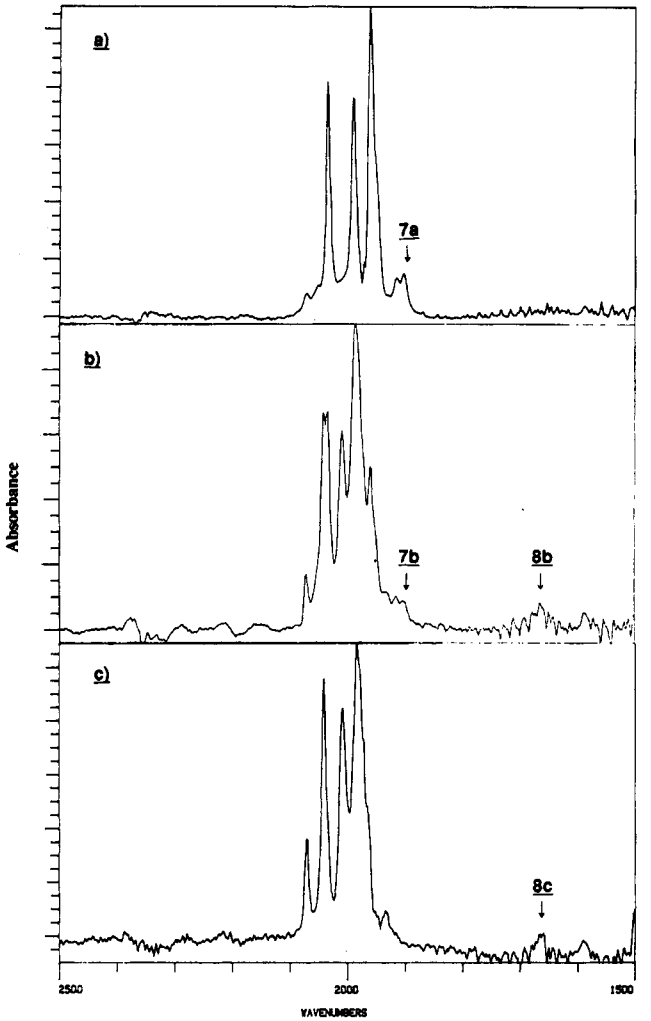

Figure 2. Infrared spectral comparison of $[PPN][Os_3(\mu_3\text{-}NPh)(X)(CO)_9]$: (a) X = Cl; (b) X = Br; (c) X = I.

resonances attributed to the minor product. Although the exact structure of this minor species is unknown, we believe it to be the isomer **7c** shown in eq 3 on the basis of the results summarized below for the bromo derivative. Both elemental and mass spectral analysis of the isolated product are consistent with the formula $[PPN][Os_3(\mu_3\text{-}NPh)(I)(CO)_9]$, and thus the minor product is unlikely to be a species with composition significantly different from that of **8c**.

The reactivity of **6** with bromide is intermediate between its reactivity with chloride and iodide, giving by IR spectroscopy an approximately 1:1 mixture of the isomers $[PPN][Os_3(\mu_3\text{-}NPh)(\mu_2\text{-}Br)(CO)_9]$ (**7b**) and $[PPN][Os_3(\mu_3\text{-}NPh)(Br)(CO)_9]$ (**8b**) (eq 4). This mixture of compounds was isolated in good yield (74%) as a yellow-orange microcrystalline solid, but the separation of these two salts has not been achieved. Evidence for the presence of both compounds came from the IR spectrum of the product mixture, shown in Figure 2, which is a composite of the IR spectra characteristic of compounds **7a** and **8c**. A band at 1665 cm^{-1} clearly indicates the presence of a triply bridging CO ligand and hence the presence of isomer **8b**, and weak absorptions at 1910 and 1900 cm^{-1} are similar to the weak bands at these positions observed in the spectrum of **7a**. In an attempt to change the isomer ratio, the product mixture was heated at 40 °C overnight in THF solution under N_2, but IR analysis indicated no significant change in the isomer distribution, although some decomposition did occur.

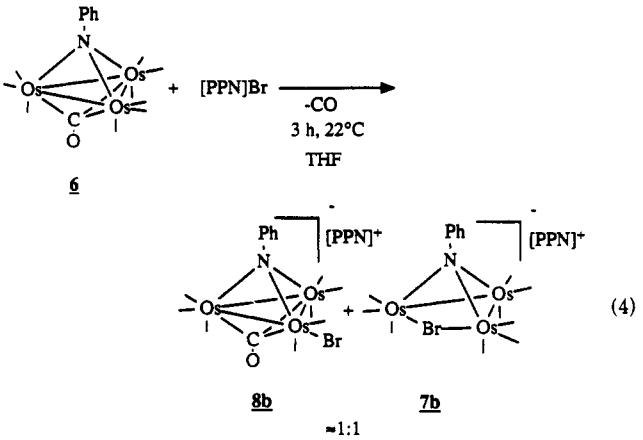

Since the phenylimido cluster **6** and its derivatives lack convenient ^1H NMR signals to monitor, the analogous tolylimido cluster $Os_3(\mu_3\text{-}NTol)(CO)_{10}$ (**6′**) was prepared by appropriate modification of the published procedure for **6**.[4] This new derivative has been characterized spectroscopically (see Experimental Section), and the data thus obtained are consistent with a structure identical to that of the phenylimido cluster **6**. The reactions of **6′** with halides proceed similarly to those of **6** to give isomeric halide substituted products **7′** and **8′** (eq 5). The ^1H NMR

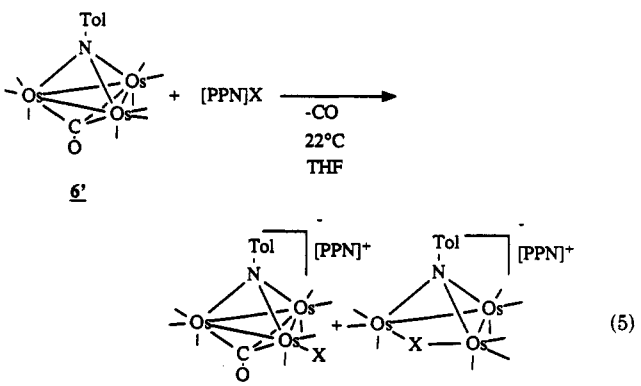

X=	8′:7′(by ^1H NMR)
Cl	< 0.1
Br	~1
I	>10

data summarized in the Experimental Section indicate that **7′** and **8′** form in ratios similar to those seen in the phenylimido reactions. Evidence that an equilibrium exists between the isomeric products **7b′** and **8b′** was obtained by dividing one sample of the mixture into two portions and then dissolving one portion in THF-d_8 and the other in CD_2Cl_2. The ^1H NMR spectrum of the THF-d_8 solution showed a ~1:1 ratio of the tolyl methyl resonances due to **7b′** and **8b′**, whereas in CD_2Cl_2 these two resonances appeared in a ~1:2 ratio, indicating that the position of the equilibrium is solvent sensitive.

Protonation Reactions. Cluster **7a** was observed to undergo clean protonation to give the hydride cluster **9a** (eq 6), which was isolated in 84% yield and has been spectroscopically characterized. It showed a molecular ion in its FAB mass spectrum and a ^1H NMR singlet at δ −12.19 for the bridging hydride ligand. Its IR spectrum in the ν_{CO} region is similar to the spectra of the double-bridged clusters $M_3(\mu_2\text{-}H)_2(\mu_3\text{-}NR)(CO)_9$ (M = Ru, Os),[9]

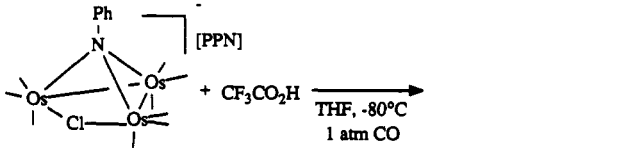

7a

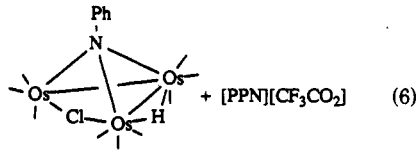

(6)

9a

suggesting that both the hydride and the chloride ligands are in bridging positions. The −73 °C ^{13}C NMR spectrum of **9a** showed nine resonances between δ 164–187 integrating to one carbon each and assigned to the nine inequivalent terminal carbonyl ligands in the proposed structure.

Also formed in low yield in the protonation reaction was the known compound $Os_3(\mu_2\text{-}Cl)(\mu_2\text{-}H)(CO)_{10}$[10] and the new isomeric μ_2-amido clusters **10a** and **11a** which differ only

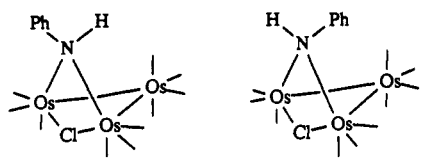

10a (*exo*) **11a** (*endo*)

in the exo/endo orientation of the amido substituents. These two species were obtained in higher, but inconsistent, yields when the protonation was conducted using $HBF_4 \cdot Et_2O$ (see Experimental Section), and both compounds were crystallographically characterized. Clusters **10a** and **11a** are discrete compounds which do not readily interconvert since pure samples of both isomers were stable in CD_2Cl_2 solutions for days. One possible mode for their interconversion would involve deprotonation of the amido ligand, but it was observed that the N–H protons of **10a** and **11a** did not incorporate deuterium when the compounds were stirred in the presence of D_2O for several days and that the chemical shift of the N–H ^1H NMR resonances showed no concentration dependence. These observations indicate that the amido protons of **10a** and **11a** are not readily removed, consistent with the fact that these compounds do not interconvert.

ORTEP drawings of the isomeric clusters **10a** and **11a** are shown in Figures 3 and 4, and pertinent crystallographic details are given in Tables I and IV–VII. Each of the molecules has two Os–Os bonds of typical single bond lengths (average 2.861 [1] Å),[6] which compare to the average Os–Os bond length of 2.8771 [27] Å[6,11] in $Os_3(CO)_{12}$. The two nonbonded Os atoms in each compound (average Os···Os = 3.156 [3] Å)[6] are symmetrically bridged by the chloride and the amido ligands. The Os–Cl (average 2.490 [1] Å)[6] and the Os–N (average 2.176 [6] Å)[6] bond lengths in the two compounds are similar as are the Os–Cl–Os (average 78.6 [0]°)[6] and Os–N–Os (average 93.0 [1]°)[6] bond angles. The orientation of the phenyl group differs considerably in the two isomers, with the N–H bond of **10a** lying in the plane of phenyl ring while the N–H bond of **11a** is approximately perpendicular to the plane of the phenyl ring (see Figures 3 and 4).

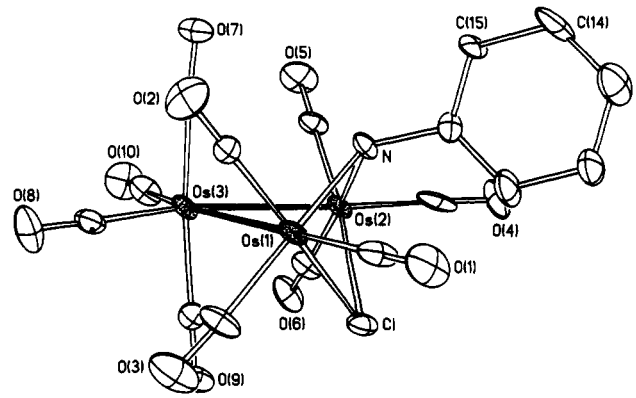

Figure 3. ORTEP drawing of $Os_3(exo\text{-}\mu_2\text{-}N(H)Ph)(\mu_2\text{-}Cl)(CO)_{10}$ (**10a**). Thermal ellipsoids are drawn at the 35% probability level.

Table IV. Atomic Coordinates (×10⁴) and Isotropic Thermal Parameters (Å² × 10³) for $Os_3(exo\text{-}\mu_2\text{-}N(H)Ph)(\mu_2\text{-}Cl)(CO)_{10}$ (10a)

	x	*y*	*y*	U^a
Os(1)	3718.0 (6)	212.2 (5)	774.6 (5)	47.3 (4)
Os(2)	2086.0 (6)	190.8 (5)	−1168.2 (5)	48.0 (4)
Os(3)	2310.5 (6)	−979.0 (5)	96.0 (6)	50.0 (4)
Cl	3805 (4)	164 (4)	−612. (4)	55 (2)
N	2655. (14)	1029 (10)	−110 (11)	55 (8)
O(1)	3275 (13)	150 (10)	2281 (10)	69 (8)
O(2)	5250 (15)	1448 (13)	1707 (14)	94 (11)
O(3)	5088 (11)	−1101 (11)	1637 (12)	80 (9)
O(4)	69 (12)	93 (12)	−1580 (11)	76 (9)
O(5)	1601 (16)	1341 (14)	−2677 (13)	109 (12)
O(6)	1682 (16)	−1157 (12)	−2446 (14)	96 (12)
O(7)	1128 (13)	32 (12)	650 (12)	76 (9)
O(8)	659 (13)	−1956 (13)	−1166 (13)	90 (11)
O(9)	3038 (15)	−1961 (12)	1761 (14)	96 (12)
O(10)	3608 (15)	−1759 (11)	−496 (14)	85 (11)
C(1)	3449 (13)	168 (15)	1687 (12)	55 (9)
C(2)	4644 (19)	955 (20)	1252 (17)	84 (14)
C(3)	4595 (13)	−607 (15)	1317 (16)	56 (10)
C(4)	841 (15)	129 (12)	−1404 (12)	44 (9)
C(5)	1850 (20)	960 (16)	−2080 (17)	76 (13)
C(6)	1819 (18)	−646 (16)	−1954 (16)	71 (12)
C(7)	1614 (17)	−307 (12)	473 (14)	54 (10)
C(8)	1271 (18)	−1595 (15)	−718 (18)	69 (13)
C(9)	2734 (18)	−1564 (14)	1144 (16)	64 (12)
C(10)	3110 (23)	−1473 (14)	−289 (16)	77 (16)
C(11)	2460 (10)	1806 (9)	1014 (9)	60 (11)
C(12)	1944	2305	1257	84 (18)
C(13)	1031	2507	651	116 (28)
C(14)	633	2210	−197	95 (19)
C(15)	1149	1711	−440	97 (18)
C(16)	2062	1509	166	57 (12)

[a] Equivalent isotropic U defined as one-third of the trace of the orthogonalized U_{ij} tensor.

Table V. Selected Bond Distances and Bond Angles for $Os_3(exo\text{-}\mu_2\text{-}N(H)Ph)(\mu_2\text{-}Cl)(CO)_{10}$ (10a)

(a) Bond Distances (Å)

Os(1)–Os(3)	2.863 (1)	Os(2)–Cl	2.488 (6)
Os(2)–Os(3)	2.863 (1)	Os(1)–N	2.182 (16)
Os(1)···Os(2)	3.152 (1)	Os(2)–N	2.161 (16)
Os(1)–Cl	2.488 (7)	N–C(16)	1.510 (30)

(b) Bond Angles (deg)

Os(3)–Os(1)–Cl	88.9 (1)	Os(1)–Os(3)–Os(2)	66.8 (1)
Os(3)–Os(1)–N	87.3 (5)	Os(1)–Cl–Os(2)	78.6 (2)
Cl–Os(1)–N	74.3 (6)	Os(1)–N–Os(2)	93.0 (7)
Os(3)–Os(2)–Cl	88.9 (1)	Os(1)–N–C(16)	122.3 (12)
Os(3)–Os(2)–N	87.7 (5)	Os(2)–N–C(16)	123.5 (12)
Cl–Os(2)–N	74.6 (6)		

(9) (a) Bhaduri, S.; Gopalkrishnan, K. S.; Clegg, W.; Jones, P. G.; Sheldrick, G. M.; Stalke, D. *J. Chem. Soc., Dalton Trans.* **1984**, 1765. (b) Lin, Y. C.; Knobler, C. B.; Kaesz, H. D. *J. Organomet. Chem.* **1981**, *213*, C41. (c) Burgess, C. K.; Johnson, B. F. G.; Lewis, J.; Raithby, P. R. *J. Chem. Soc., Dalton Trans* **1982**, 2085.

(10) Bryan, E. G.; Johnson, B. F. G.; Lewis, J. *J. Chem. Soc., Dalton Trans.* **1977**, 1328.

(11) Churchill, M. R.; DeBoer, B. G. *Inorg. Chem.* **1977**, *16*, 878.

Table VI. Atomic Coordinates (×10⁴) and Isotropic Thermal Parameters (Å² × 10³) for Os_3(*endo*-μ_2-N(H)Ph)(μ_2-Cl)$(CO)_{10}$ (11a)

	x	y	z	U[a]
Os(1)	1492.8 (4)	1122.5 (6)	863.8 (6)	31.5 (3)
Os(2)	882.8 (3)	-954.9 (6)	949.1 (6)	30.5 (2)
Os(3)	1803.6 (4)	-703.2 (6)	-221.1 (6)	30.5 (2)
Cl	624 (2)	734 (4)	199 (4)	43 (2)
O(1)	1175 (9)	3090 (13)	2000 (15)	78 (8)
O(2)	2581 (7)	1306 (14)	1596 (16)	70 (8)
O(3)	1801 (9)	2366 (15)	-1095 (16)	81 (9)
O(4)	-77 (7)	-1205 (16)	2320 (14)	70 (7)
O(5)	1328 (8)	-2871 (12)	1774 (16)	70 (8)
O(6)	480 (8)	-2154 (13)	-958 (14)	65 (7)
O(7)	2397 (7)	-1241 (14)	1820 (14)	63 (7)
O(8)	2709 (7)	339 (15)	-1275 (16)	76 (8)
O(9)	1102 (7)	-101 (11)	-2079 (14)	59 (7)
O(10)	1878 (8)	-2895 (12)	-1088 (16)	75 (8)
N	1247 (7)	46 (12)	2107 (13)	34 (6)
C(1)	1275 (11)	2365 (16)	1589 (17)	53 (9)
C(2)	2186 (8)	1243 (16)	1320 (17)	33 (5)
C(3)	1674 (10)	1916 (18)	-390 (18)	47 (9)
C(4)	313 (12)	-1056 (15)	1805 (18)	58 (10)
C(5)	1170 (10)	-2148 (15)	1478 (17)	41 (8)
C(6)	619 (10)	-1691 (17)	-264 (19)	47 (9)
C(7)	2193 (8)	-1023 (16)	1044 (18)	40 (5)
C(8)	2364 (9)	-47 (17)	-888 (18)	44 (8)
C(9)	1359 (8)	-326 (18)	-1383 (18)	40 (5)
C(10)	1852 (10)	-2053 (16)	-764 (19)	48 (8)
C(11)	528 (6)	1014 (12)	2941 (10)	63 (11)
C(12)	263	1319	3856	68 (11)
C(13)	417	981	4868	72 (13)
C(14)	836	339	4965	72 (13)
C(15)	1101	34	4050	47 (9)
C(16)	947	371	3038	35 (7)

[a] Equivalent isotropic U defined as one-third of the trace of the orthogonalized U_{ij} tensor.

Table VII. Selected Bond Distances and Bond Angles for Os_3(*endo*-μ_2-N(H)Ph)(μ_2-Cl)$(CO)_{10}$ (11a)

(a) Bond Distances (Å)

Os(1)–Os(3)	2.862 (1)	Os(2)–Cl	2.492 (6)
Os(2)–Os(3)	2.855 (1)	Os(1)–N	2.190 (16)
Os(1)···Os(2)	3.159 (1)	Os(2)–N	2.171 (16)
Os(1)–Cl	2.493 (6)	N–C(16)	1.467 (22)

(b) Bond Angles (deg)

Os(3)–Os(1)–Cl	86.4 (1)	Os(1)–Os(3)–Os(2)	67.1 (1)
Os(3)–Os(1)–N	83.3 (4)	Os(1)–Cl–Os(2)	78.6 (2)
Cl–Os(1)–N	80.2 (5)	Os(1)–N–Os(2)	92.9 (6)
Os(3)–Os(2)–Cl	86.6 (1)	Os(1)–N–C(16)	122.1 (11)
Os(3)–Os(2)–N	83.8 (5)	Os(2)–N–C(16)	117.4 (12)
Cl–Os(2)–N	80.6 (4)		

The iodide-substituted cluster **8c** undergoes similar, but slower, protonation to give **9c** as the major product (eq 7).

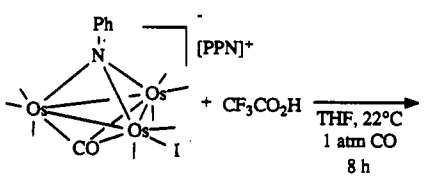

8c

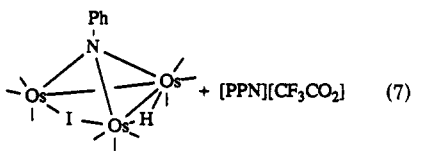

(7)

9c (32%)

Its spectroscopic data summarized in the Experimental Section are similar to those of **9a** and indicate a similar structure. Also isolated from this reaction in low yields

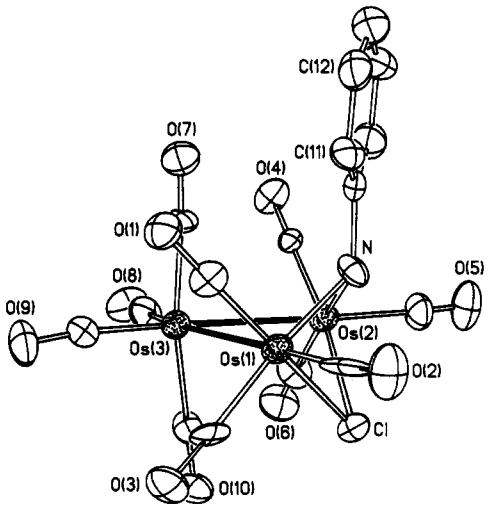

Figure 4. ORTEP drawing of Os_3(*endo*-μ_2-N(H)Ph)(μ_2-Cl)$(CO)_{10}$ (**11a**). Thermal ellipsoids are drawn at the 35% probability level.

were the known complex $Os_3(\mu_2\text{-H})(\mu_2\text{-I})(CO)_{10}$[12] and the new μ_2-amido clusters Os_3(*exo*-μ_2-N(H)Ph)(μ_2-I)$(CO)_{10}$ (**10c**) and Os_3(*endo*-μ_2-N(H)Ph)(μ_2-I)$(CO)_{10}$ (**11c**), for which spectroscopic data indicate structures analogous to those of **10a** and **11a**. The IR spectra of the exo compounds **10a** and **10c** are essentially identical in the ν_{CO} region, and their ^{1}H NMR spectra showed broad resonances assigned to the protons of the μ_2-amido ligands at δ 3.64 (**10a**) and 3.88 (**10c**). Likewise, the IR spectra of the endo compounds **11a** and **11c** are similar, although less so than in the case of the exo compounds, and their ^{1}H NMR spectra showed broad resonances at δ 5.17 (**11a**) and 4.73 (**11c**) assigned to the protons of the μ_2-amido ligands. The EI mass spectrum of **10c** showed a peak at m/z = 1070 corresponding to the mass of **10c** minus one proton, and the EI mass spectrum of **11c** showed a molecular ion peak at m/z = 1071. Additionally, the chromatographic behavior of **10c** was similar to that of **10a** as was that of **11c** to **11a**.

Carbonylation Reactions. The parent imido cluster $Os_3(\mu_3\text{-NPh})(CO)_{10}$ (**6**) is resistant to carbonylation, giving no reaction after 4 h at 65 °C under 82 atm of CO in THF solution. In contrast, complex **7a** slowly reacts with CO at room temperature to yield a mixture of the new μ-phenyl isocyanate cluster $[Os_3(\eta^2\text{-}\mu_2\text{-PhNCO})(\mu_2\text{-Cl})(CO)_{10}]^-$ (**13a**) and the known cluster $[Os_3(Cl)(CO)_{11}]^-$[13] (**14a**) (eq 8). The optimum reaction time for the maximum yield of **13a** was 93 h. Shorter reaction times left

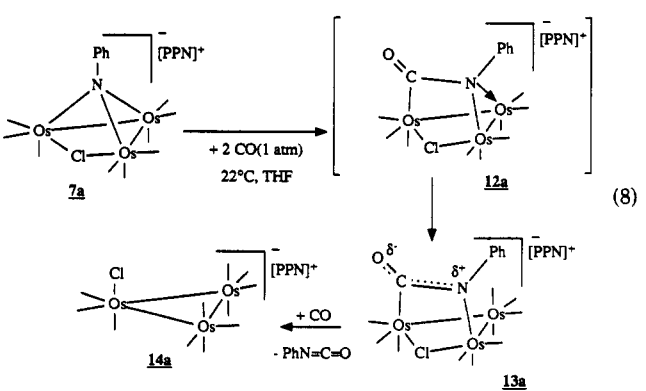

(8)

(12) Bryan, E. G.; Foster, A.; Johnson, B. F. G.; Lewis, J.; Matheson, T. W. *J. Chem. Soc., Dalton Trans* **1978**, 196.
(13) Zuffa, J. L.; Kivi, S. J.; Gladfelter, W. L. *Inorg. Chem.* **1989**, *28*, 1888.

more **7a**, and longer reaction times induced more elimination of PhN=C=O (detected by IR) from **13a** to form **14a**. Despite numerous variations in the reaction time, temperature, and carbon monoxide pressure, conditions were not found that would allow the isolation of **13a** in pure form, and mixtures containing two or more of **7a**, **13a**, and **14a** were always obtained. Although we have been unable to obtain spectroscopic evidence for the intermediate **12a**, a corresponding compound has been detected in the reactions of the iodide-substituted arylimido analogues **8c** and **8c'** with CO (see below).

The formulation of the new cluster **13a** was made on the basis of its spectroscopic data. Also supporting its assigned structure are the alkylation reactions described in the following section. The negative ionization FAB mass spectrum of the mixture of compounds from reaction 8 showed a strong molecular ion at m/z = 1006, consistent with the proposed formulation for **13a**, as well as a ten carbonyl loss pattern. The IR spectrum of the mixture of products obtained at 93 h carbonylation time, when the concentration of **13a** was at its highest, showed only bands due to terminal carbonyl ligands. No absorption was apparent which could be unambiguously assigned to the carbonyl group of the η^2-μ_2-PhNCO ligand. This is in contrast to the 1610-cm^{-1} band reported for the η^2-μ_3-PhNCO ligand in the cluster $[Ru_3(\mu_2\text{-H})(\eta^2\text{-}\mu_3\text{-PhNCO})(CO)_9]^-$ (**15**).[14] The absence of a comparable band in **13a**

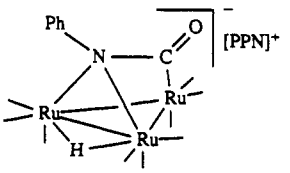

15

may be attributed to the lowering of the CO bond order and its corresponding frequency into the region obscured by the phenyl substituent and the $[PPN]^+$ counterion by delocalization of the nitrogen lone pair, illustrated as follows:

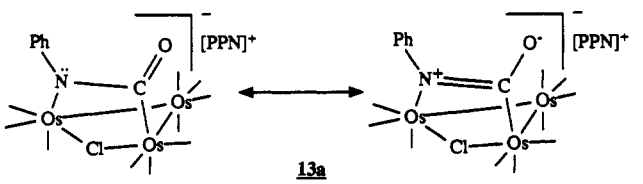

13a

Note that in **15** this electron pair is tied up through bonding to the third metal atom, but it is not in **13a**. For comparison, the crystallographically characterized compound $Rh_2(dppm)_2(\eta^2\text{-}\mu_2\text{-PhNCO})(CO)_2$ also failed to show an identifiable ν(CO) band.[15] The IR stretch of the ketene complex $[PPN][Os_3(\eta^2\text{-}\mu_2\text{-}CH_2CO)(Cl)(CO)_{10}]$, which is isoelectronic and isostructural with **13a**, was observed at 1556 cm^{-1}.[16]

The −73 °C ^{13}C NMR spectrum of the mixture of products from reaction 8 contains too many peaks in the terminal carbonyl region (δ 189–166) to allow an accurate assignment, but one resonance is apparent at δ 198.9 which does not belong to either **7a** or **14a** and is outside the normal range of terminal osmium carbonyl ligands. A thorough analysis of 50 Os_3 clusters for which we could find reported ^{13}C NMR data identified the range of δ 167.0–194.4 for the most downfield resonance of each compound with a mean value of δ 183.2 (see Table A of the supplementary material). All of these resonances lie within $\pm 2\sigma_{n-1}$ of the mean except for the resonances of $Os_3(\mu_3\text{-}COCH_3)(\mu_2\text{-H})_3(CO)_9$[17a] and $Os_3(\mu_3\text{-}CCH_3)(\mu_2\text{-H})(CO)_9$,[17b] which appear at δ 167.0 and δ 167.6, respectively. The δ 198.9 resonance of **13a** is 3.9 ppm outside the $\pm 2\sigma_{n-1}$ range, and we thus conclude that this resonance is not due to a carbonyl ligand but is instead assigned to the carbonyl group of the η^2-μ_2-PhNCO ligand. For comparison, the ^{13}C NMR resonance for the η^2-μ_2-PhNCO ligand in $Rh_2(dppm)_2(\eta^2\text{-}\mu_2\text{-PhNCO})(CO)_2$ is at δ 206, just slightly downfield from the resonance assigned to the isocyanate ligand in **13a**.

In the course of these studies, a sample of the analogous tolyl isocyanate cluster **13a'*** was prepared in which the carbonyl ligands and the tolyl isocyanate ligand carbonyl carbon were >50% enriched in ^{13}C and which proved to be >75% pure by ^{13}C NMR spectroscopy. Thus, the ^{13}C NMR spectrum was more interpretable since the impurity peaks were small relative to those of **13a'***. The −63 °C ^{13}C NMR spectrum of this sample showed two doublets at δ 198.1 and 187.9, each with $^2J_{CC}$ = 29.0 Hz. This coupling constant is a typical value for two-bond trans C–C coupling across Os,[18] and these two resonances are respectively assigned to the tolyl isocyanate carbonyl carbon and carbonyl ligand *a*, shown as

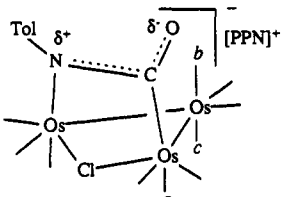

13a'*

Two other doublets, each with $^2J_{CC} \sim 33$ Hz, were additionally observed, and these are assigned to the trans carbonyl ligands *b* and *c*.

The iodo complex **8c** undergoes a similar reaction with CO to form a mixture of the starting cluster **8c**, the new μ-PhNCO clusters $[Os_3(\eta^2\text{-}\mu_3\text{-PhNCO})(\mu_2\text{-I})(CO)_9]^-$ (**12c**) and $[Os_3(\eta^2\text{-}\mu_2\text{-PhNCO})(\mu_2\text{-I})(CO)_{10}]^-$ (**13c**), and the known cluster $[Os_3(I)(CO)_{11}]^-$ (**14c**)[13] (eq 9). It is significant that

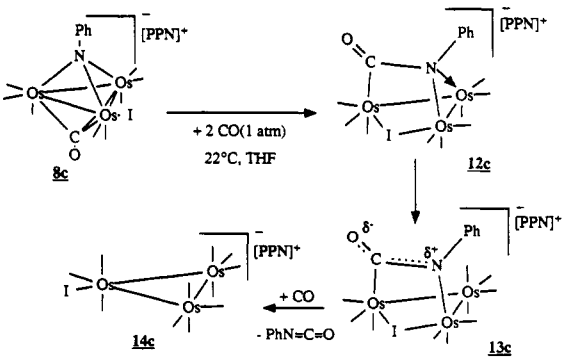

(9)

this reaction required only 14 h for the maximum yield of **13c**, in contrast to the 93 h required for **13a** under similar pressure and temperature conditions. As above, the re-

(14) Bhaduri, S.; Khwaja, H.; Jones, P. G. *J. Chem. Soc., Chem. Commun.* **1988**, 194.
(15) Ge, Y.-W.; Sharp, P. R. *Organometallics* **1988**, *7*, 2234.
(16) Morrison, E. D.; Geoffroy, G. L. *J. Am. Chem. Soc.* **1985**, *107*, 3541.
(17) (a) Keister, J. B.; Payne, M. W.; Muscatella, M. J. *Organometallics* **1983**, *2*, 219. (b) Forster, Alison; Johnson, B. F. G.; Lewis, J.; Matheson, T. W. *J. Organomet. Chem.* **1976**, *104*, 225.
(18) Shapley, J. R.; Cree-Uchiyama, M. E.; St. George, G. M. *J. Am. Chem. Soc.* **1983**, *105*, 140.

action would always give a mixture of products and no conditions were found which gave pure samples of **12c** or **13c**. The new cluster **13c** was characterized by its spectroscopic data and especially by the alkylation reaction described below. The product mixture showed a strong molecular ion at m/z = 1098 for **13c** in its negative ionization FAB mass spectrum. The IR spectrum of the reaction mixture showed only terminal ν(CO) bands, but as in the chloride case, no band was identified which could be confidently assigned to the η^2-μ_2-PhNCO ligand. The −73 °C ^{13}C NMR spectrum of the product mixture showed a resonance at δ 198.5, which is attributed to the carbonyl carbon of the isocyanate ligand. A sample of ^{13}C-enriched **13c**, designated **13c***, was prepared from ~50% ^{13}C-en-

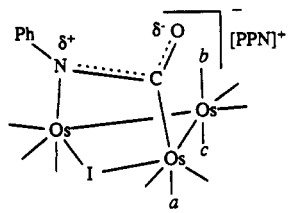

13c

riched **8c*** (see Experimental Section) by stirring the latter in THF solution under 1 atm of ^{13}CO (99%). The resonance assigned to the isocyanate carbon of **13c*** appeared as a doublet superimposed upon a singlet, due to incomplete ^{13}C incorporation into the trans carbonyl, with $^2J_{CC}$ = 30 Hz, a typical value for two-bond ^{13}C–^{13}C trans coupling.[18] Additionally, 2D ^{13}C–^{13}C COSY and 2D INADEQUATE experiments showed that this resonance is coupled to a resonance at δ 182.2 and that a resonance at δ 187.3 is coupled to a resonance at δ 181.4 with $^2J_{CC}$ ~ 30 Hz. Thus the resonance at δ 182.2 is assigned to carbonyl ligand *a*, which is trans to the isocyanate carbonyl, and the resonances at δ 187.3 and δ 181.4 are assigned to carbonyl ligands *b* and *c*, which are trans to each other.

Many of the details of the carbonylation reaction became more apparent through work with the analogous tolylimido cluster **6′**, the most important of which was the identification of **12′** as an intermediate in the carbonylation reaction between **7′** or **8′** and **13′**. It was found by ^{1}H NMR spectroscopy that **7a′** and **8c′** could be obtained cleanly only when steps were taken to ensure that the CO liberated in the halide substitution reaction was not allowed to accumulate. This was achieved by the use of a continuous nitrogen purge through the solution kept at 23 °C by a thermostatic bath. In contrast, when **6′** and [PPN]I were dissolved in THF-d_8 in a sealed NMR tube from which the released CO could not escape, a ~3:1 mixture of **8c′** (δ 2.25, tolyl CH_3) and a new species formulated as [PPN][Os_3-(η^2-μ_3-TolNCO)(μ_2-I)(CO)$_9$] (**12c′**) (δ 2.34, tolyl CH_3), was produced (eq 10). Proton NMR monitoring showed that

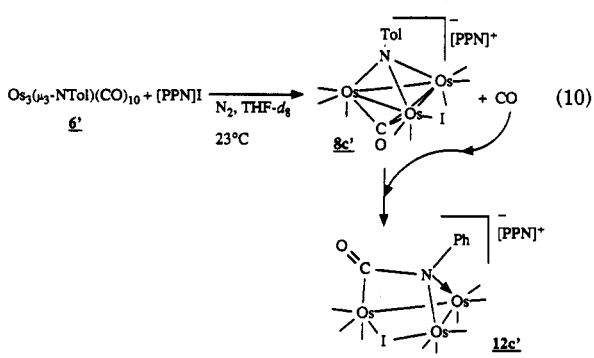

cluster **8c′** initially formed and then resonances for **12c′** grew in until an apparent equilibrium was reached. When this solution was degassed by three freeze/pump/thaw cycles and then back-filled with 1 atm of CO, conversion of most of the remaining **8c′** to **12c′** occurred within 24 h, and some **13c′** (δ 2.30, tolyl CH_3) was also observed. It should be noted that the rates of both the substitution and carbonylation reactions are highly dependent upon the rate (or absence) of stirring since this is a three-phase system with CO in the gas and solution phases, and the [PPN]X salt, which is only slightly soluble in THF, is present in both the solid and solution phases. Therefore, the rates of reactions performed in an unstirred NMR tube are not comparable to those obtained in a vigorously stirred solution in a Schlenk flask. Additionally, when the volume of the gas phase is small in relation to the volume of the solution phase and when the concentration of the Os_3 cluster in solution is high, as in a typical NMR tube experiment, an insufficient amount of CO is present to form **13′**, and this permitted the detection of **12′**. In experiments in Schlenk flasks under flowing CO, which ensured a constant concentration of CO throughout the duration of the reaction, **7′** and **8′** carbonylate to give mostly **13′** with little or no **12′** detected.

Clusters **12c** and **12c′** have been characterized by their −63 °C ^{13}C NMR spectra. Each showed resonances in CD_2Cl_2 assigned to the η^2-μ_3-PhNCO ligand (**12c**, δ 193.7; **12c′**, δ 193.8) along with nine resonances of equal intensity in the terminal Os carbonyl region which are assigned to the nine inequivalent carbonyl ligands of the proposed structure. A sample containing ^{13}C-labeled **12c′*** exhibited in THF-d_8 a doublet at δ 192.3 with $^2J_{CC}$ = 29 Hz, but a significant amount of **13c′*** was also present and prevented any further interpretation.

Protonation and Alkylation of the Phenyl Isocyanate Ligand in [$Os_3(\eta^2\text{-}\mu_2\text{-PhNCO})(\mu_2\text{-X})(CO)_{10}$]$^-$. In an attempt to convert the anionic η^2-μ_2-PhNCO clusters **13a** and **13c** into neutral compounds which could be more readily separated from their coproducts, the product mixture was treated with alkylating and protonating agents. The alkylation reactions are discussed first since they led to the cleanest products. When treated with methyl triflate at −80 °C under 1 atm of CO, the mixtures of compounds from the carbonylation reactions 8 and 9 gave as the major products the clusters $Os_3(\eta^2\text{-}\mu_2$-PhNCOCH$_3$)(μ_2-X)(CO)$_{10}$ (**17**) (eq 11). Alkylation under

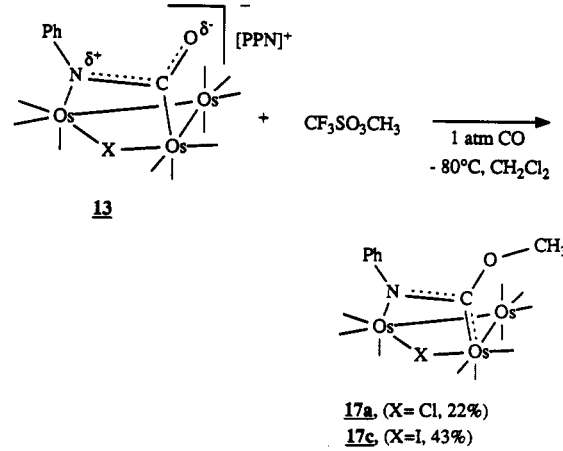

an N_2 atmosphere led to similar yields. Both **17a** and **17c** were isolated as microcrystalline solids, and **17c** was crystallographically characterized. An ORTEP drawing of **17c** is shown in Figure 5, and relevant crystallographic data are set out in Tables I, VIII, and IX. The metal atoms form an open triangle with two Os–Os single bonds (2.897 and 2.899 Å). The nonbonded osmium atoms are separated by 3.570 (2) Å and are bridged by the η^2-μ_2-

Table VIII. Atomic Coordinates (×10⁴) and Isotropic Thermal Parameters (Å² × 10³) for $Os_3(\mu_2\text{-PhNCOCH}_3)(\mu_2\text{-I})(CO)_{10}$ (17c)

	x	y	z	U[a]
Os(1)	1711.8 (5)	3620.6 (7)	1014.7 (7)	53.9 (4)
Os(2)	2103.1 (6)	3417 (8)	3249.5 (7)	63.4 (5)
Os(3)	1674.4 (6)	4887.5 (8)	2193.7 (7)	60.6 (5)
I	2816 (1)	2956 (1)	2308 (1)	73 (1)
N	1164 (11)	2803 (14)	1480 (14)	66 (10)
O(1)	1743 (11)	2356 (16)	-282 (15)	94 (12)
O(2)	455 (12)	4405 (16)	-254 (14)	92 (11)
O(3)	2560 (12)	4814 (17)	525 (17)	96 (13)
O(4)	2594 (17)	1888 (17)	4365 (19)	127 (18)
O(5)	1271 (12)	4111 (16)	4092 (12)	93 (11)
O(6)	3256 (11)	4479 (17)	4398 (16)	105 (13)
O(7)	1146 (11)	6236 (13)	794 (14)	88 (11)
O(8)	3120 (11)	5209 (18)	2517 (17)	109 (13)
O(9)	1758 (16)	6018 (18)	3700 (19)	136 (17)
O(10)	251 (10)	4205 (17)	1776 (16)	99 (12)
O(11)	896 (10)	2238 (13)	2461 (13)	77 (10)
C(1)	1730 (14)	2740 (19)	260 (16)	61 (12)
C(2)	967 (15)	4130 (18)	248 (16)	59 (12)
C(3)	2247 (19)	4344 (23)	693 (21)	92 (17)
C(4)	2408 (15)	2379 (31)	3968 (18)	89 (18)
C(5)	1564 (18)	3809 (22)	3773 (20)	86 (17)
C(6)	2802 (16)	4035 (20)	3989 (21)	78 (9)
C(7)	1352 (14)	5703 (19)	1340 (15)	70 (12)
C(8)	2600 (15)	5041 (19)	2396 (16)	66 (13)
C(9)	1734 (19)	5622 (23)	3151 (24)	98 (19)
C(10)	781 (22)	4469 (22)	1946 (20)	104 (22)
C(11)	1317 (13)	2791 (20)	2354 (18)	66 (13)
C(12)	880 (19)	2198 (28)	3350 (30)	135 (27)
C(21)	896 (8)	1519 (13)	721 (14)	85 (17)
C(22)	434	1007	113	96 (21)
C(23)	-222	1267	-312	93 (20)
C(24)	-415	2039	-128	89 (16)
C(25)	48	2552	480	85 (17)
C(26)	703	2292	905	46 (11)
CS(1)	0	7610	2500	260 (55)
CS(2)	158 (26)	7372 (38)	1875 (36)	146 (18)
CS(3)	38 (30)	6568 (35)	1942 (37)	158 (20)
CS(4)	622 (26)	9791 (34)	3212 (34)	144 (18)
CS(5)	617 (35)	9592 (47)	2813 (47)	213 (28)
CS(6)	0	10006 (64)	2129 (69)	354 (64)

[a] Equivalent isotropic U defined as one-third of the trace of the orthogonalized U_{ij} tensor.

PhNCOMe and the μ_2-I ligands. The PhNCOMe ligand is essentially planar with a N–C(11) bond length of 1.39 (2) Å. This is substantially longer than the N=C bond length of 1.27 Å found in $Os_3(\eta^2\text{-}\mu_2\text{-MeN=COC(O)N(H)Me})(\mu_2\text{-H})(CO)_{10}$ (18).[19] In contrast, the C(11)–Os(2) bond

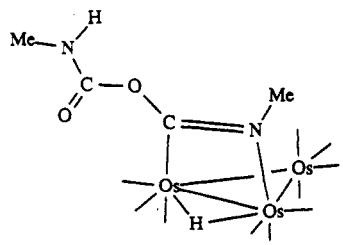

18

length of 2.05 (2) Å in 17c is shorter than the C–Os bond length of 2.13 Å in 18, and the Os(1)–N bond length in 17c (2.15 (2) Å) is longer than the Os–N bond length of 18. The doubly-bridged Os–Os bond in 18 is much shorter (2.924 Å) than the Os(1)···Os(2) distance in 17c. This comparison

(19) Lin, Y.-C.; Mayr, A.; Knobler, C. B.; Kaesz, H. D. *J. Organomet. Chem.* **1984**, *272*, 207.

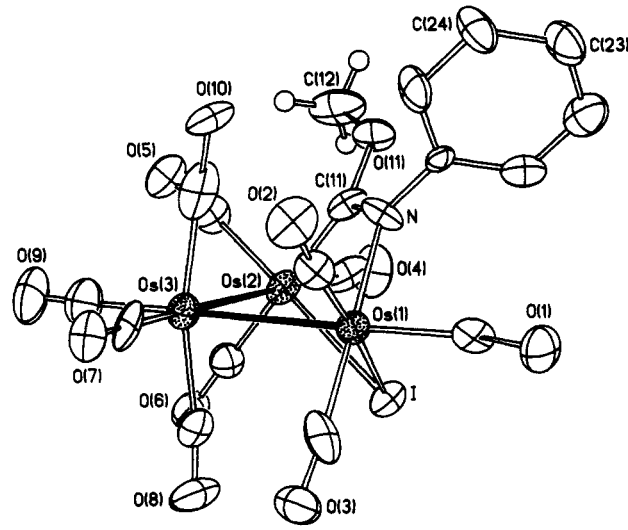

Figure 5. ORTEP drawing of $Os_3(\mu_2\text{-PhNCOMe})(\mu_2\text{-I})(CO)_{10}$ (17c). Thermal ellipsoids are drawn at the 35% probability level.

suggests delocalized bonding in 17c, as indicated by the following resonance forms:

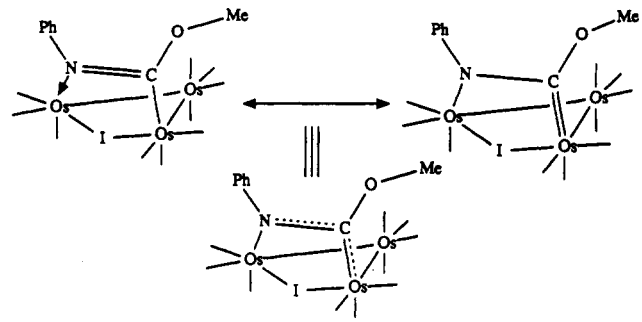

The η^2-μ^2-PhNCO ligands of 13a and 13c also undergo protonation with CF_3CO_2H to form the clusters $Os_3(\mu_2\text{-PhNCOH})(\mu_2\text{-X})(CO)_{10}$ (19a,c) (eq 12). These clusters

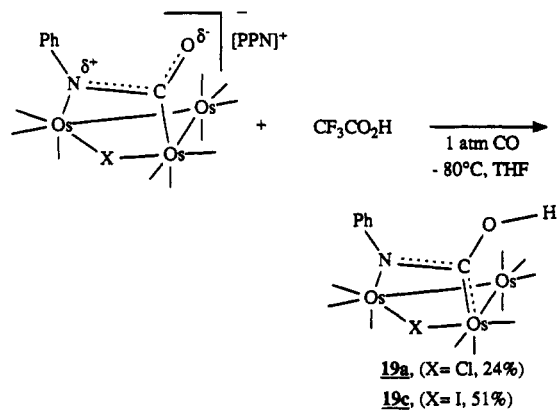

19a, (X= Cl, 24%)
19c, (X= I, 51%)

(12)

are similar to the known cluster $Os_3(\eta^2\text{-}\mu_2\text{-MeNCOH})(\mu_2\text{-H})(CO)_{10}$ (20), which was shown by Kaesz to be in equilibrium with 21 via a keto/enol-like tautomerization (eq 13).[19] However, an important difference between 19

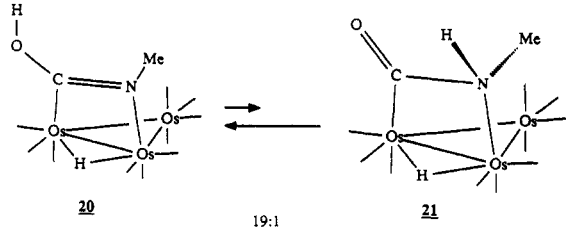

20 19:1 21

(13)

and 20 is that 19a and 19c are 50e⁻ clusters bridged by a

Table IX. Selected Bond Distances and Bond Angles for $Os_3(\mu_2\text{-}PhNCOCH_3)(\mu_2\text{-}I)(CO)_{10}$ (17c)

(a) Bond Distances (Å)			
Os(1)–Os(3)	2.896 (2)	Os(2)–C(11)	2.053 (26)
Os(2)–Os(3)	2.898 (2)	N–C(11)	1.390 (38)
Os(1)···Os(2)	3.570 (2)	N–C(26)	1.368 (27)
Os(1)–I	2.757 (2)	O(11)–C(11)	1.356 (40)
Os(2)–I	2.773 (3)	O(11)–C(12)	1.536 (59)
Os(1)–N	2.151 (26)		
(b) Bond Angles (deg)			
Os(3)–Os(1)–I	89.1 (1)	Os(1)–N–C(11)	118.6 (18)
Os(3)–Os(1)–N	89.8 (7)	Os(1)–N–C(26)	118.1 (18)
I–Os(1)–N	85.0 (5)	C(11)–N–C(26)	123.2 (25)
Os(3)–Os(2)–I	88.7 (1)	Os(2)–C(11)–N	123.7 (23)
Os(3)–Os(2)–C(11)	88.7 (8)	Os(2)–C(11)–O(11)	130.1 (20)
I–Os(2)–C(11)	86.8 (10)	N–C(11)–O(11)	105.9 (21)
Os(1)–Os(3)–Os(2)	76.1 (1)	C(11)–O(11)–C(12)	117.1 (23)

halide ligand instead of a hydride as in the 48e⁻ cluster **20**. Also formed in the reaction of **13** with CF_3CO_2H were trace amounts of the clusters **9**–**11** and $Os_3(\mu_2\text{-}H)(\mu_2\text{-}X)(CO)_{10}$.[10,12] The use of $HBF_4{\cdot}Et_2O$ as the protonating agent gave higher yields of **10a,c** and **11a,c** at the expense of **19a,c**, but the yields were variable and greater decomposition was observed. Clusters **19a** and **19c** have been characterized spectroscopically and are similar to the alkylation products **17a** and **17c**. For example, the 23 °C ^1H NMR spectrum of **19a** showed a broad resonance near δ 7.8, the chemical shift of which exhibited both temperature and concentration dependence. This resonance is assigned to the CO*H* proton and integrates 1:5 with the resonances of the phenylimido protons. The resonance assigned to the CO*H* proton of **19c** showed a similar temperature and concentration dependent chemical shift (23 °C, δ ~9.6). The −73 °C ^{13}C NMR spectrum of **19a** showed 10 resonances between δ 168 and 188 which integrated to one carbon each and are assigned to the 10 inequivalent terminal carbonyl ligands of **19a**. Also observed was a resonance at δ 203.5 which is assigned to the η^2-μ_2-PhNCOH ligand and compares well to the δ 205.1 resonance of the η^2-μ_2-PhNCOMe ligand in **17c**. The ^1H NMR spectrum of newly recrystallized **19** showed weak aromatic resonances for a second compound despite the fact that the chromatographic bands of **19** were well resolved. We tentatively suggest that these weak resonances may be due to a keto tautomer similar to **21** (see eq 13).[19]

An interesting feature of compounds **17** and **19** is the restricted rotation about the Ph–N bond of the Ph–NCOR ligand as illustrated by the variable-temperature ^1H NMR spectra of **17a** shown in Figure 6. At −26 °C, the spectrum in the aromatic region consists of a pair of doublets at δ 6.94 and 7.07 due to the inequivalent ortho protons H_a and H_a', two overlapping triplets at δ 7.42 and 7.44 assigned to the inequivalent meta protons H_b and H_b', and a pseudo-triplet at δ 7.18 due to the para proton H_c.

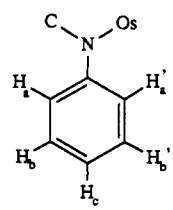

As the temperature is raised, the resonances due to the ortho and meta protons coalesce and then sharpen into averaged resonances at 43 °C. The spectra of **17c**, **19a**, and **19c** are similar to those of **17a**, and a qualitative ordering of the coalescence temperatures of **17c** > **17a** > **19c** > **19a** was observed. The restricted rotation is attributed to the partial double-bond character between the nitrogen

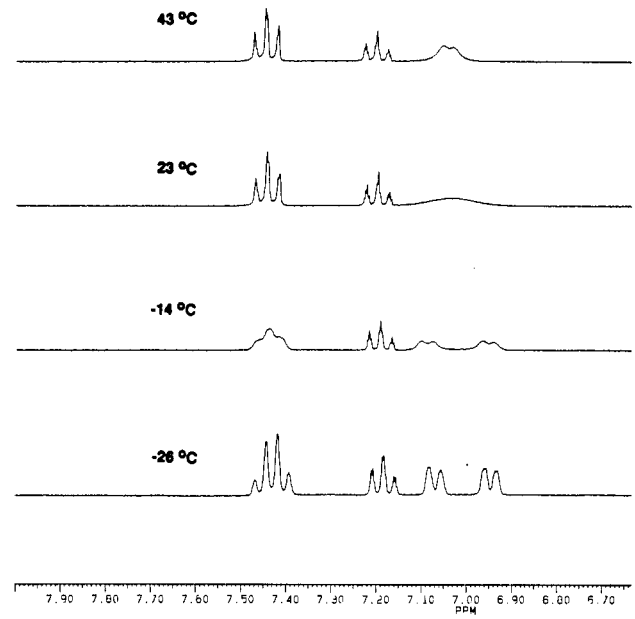

Figure 6. Variable-temperature ^1H NMR spectra of $Os_3(\eta^2\text{-}\mu_2\text{-}PhNCOCH_3)(\mu_2\text{-}Cl)(CO)_{10}$ (**17a**).

Table X. Bond Lengths (Å) of the N-*ipso*-C Bond of Compounds 7a, 10a, 11a, and 17c

compd	bond length
$[PPN][Os_3(\mu_3\text{-}NPh)(\mu_2\text{-}Cl)(CO)_9]$ (**7a**)	1.418 (12)
$Os_3(exo\text{-}\mu_2\text{-}N(H)Ph)(\mu_2\text{-}Cl)(CO)_{10}$ (**10a**)	1.510 (30)
$Os_3(endo\text{-}\mu_2\text{-}N(H)(Ph)(\mu_2\text{-}Cl)(CO)_{10}$ (**11a**)	1.467 (22)
$Os_3(\eta^2\text{-}\mu_2\text{-}PhNCOMe)(\mu_2\text{-}I)(CO)_{10}$ (**17c**)	1.368 (27)

atom and the phenyl *ipso*-carbon, and as can be seen by examination of Table X, the N–*ipso*-C bond length of **17c** is shorter than those of the other compounds crystallographically characterized in this study.

Discussion

The objective of this study was to determine if the osmium imido cluster $Os_3(\mu_3\text{-}NPh)(CO)_{10}$ (**6**) reacted with halides and with carbon monoxide in a manner similar to that of its ruthenium analogue[2] and especially to determine if intermediates could be observed in the imido carbonylation reaction. The results reported above indicate that similar reactions do occur, with some minor differences, and that carbonylation intermediates having coordinated isocyanate ligands can be observed and studied. An interesting feature of the reaction of **6** with halides is the ease with which it occurs (22 °C, 2–4 h) as compared to $Os_3(CO)_{12}$, which does not react with halides except at elevated temperatures.[13,20] The imido ligand thus activates the Os_3 framework for this substitution reaction, although it is not known how this occurs since the mechanism of the substitution has not been explored. Possibilities include CO labilization by the imido ligand, movement of the imido ligand to a μ_2-bridging position to open a coordination site for halide addition, or reduced steric crowding to allow S_N2 attack of the halide on the Os_3 framework or on a carbonyl carbon.[21]

An important difference in the reactivity of halides with $Os_3(\mu_3\text{-}NPh)(CO)_{10}$ and with $Ru_3(\mu_3\text{-}NPh)(CO)_{10}$ is that the

(20) Ramage, D. L.; Geoffroy, G. L. Unpublished observations.
(21) (a) Lavinge, G.; Kaesz, H. D. In *Metal Clusters in Catalysis*; Gates, B. C., Guczi, L., Knözinger, H., Eds.; Studies in Surface and Catalysis 29; Elsevier: New York, 1986; Chapter 4. (b) Ford, P. C.; Rokicki, A. *Adv. Organomet. Chem.* **1988**, *28*, 139. (c) Basolo, F. *Polyhedron* **1990**, *13*, 1503.

Scheme III

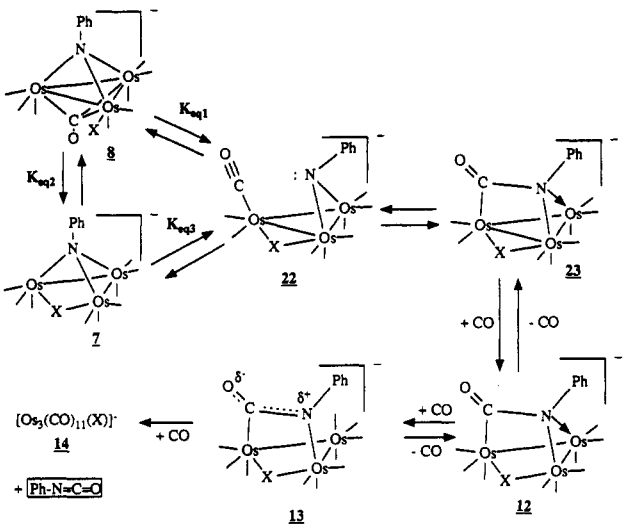

only detectable products of the latter reaction were clusters of type **2** (see Scheme I) having terminal halide ligands[2a] whereas $Os_3(\mu_3\text{-NPh})(CO)_{10}$ reacts with halides to form **7**, which possesses a bridging halide ligand, as well as **8**, which has a terminal halide and is analogous to **2**. The ratio of these products is dependent upon the halide employed, and the discussion below implies that these isomers may be in equilibrium, although we have not been able to obtain conclusive evidence for that equilibration. The shift in the isomer distribution from **7**, with a bridging halide, to **8**, with a terminal halide, as the size of the halide increases may reflect the steric constraints of the molecule, and the greater strain that may be caused by the presence of a halide bridge between two Os atoms that are also bridged by the μ_3-NPh ligand.

As was observed in the study of the analogous ruthenium clusters, halides markedly promote the carbonylation of the imido ligand in **7** and **8** since the parent cluster $Os_3(\mu_3\text{-NPh})(CO)_{10}$ is inert to carbonylation even under high-pressure, high-temperature conditions. The mechanism invoked for the carbonylation sequence is set out in Scheme III. As was proposed for the Ru_3 system,[2] we suggest that the terminal halide ligand in **8** can move to a bridging position and displace one of the Os–imido bonds to give **22**. The resulting μ_2-NPh ligand should be sufficiently basic to attack a carbonyl ligand to yield **23**. In support of this step, we note that Deeming has proposed that a similar transformation occurs during the reaction of $Os_3(\mu_2\text{-H})_2L(CO)_9$ with diazoalkanes.[22] Also, Bhaduri observed that deprotonation of $Ru_3(exo\text{-}\mu_2\text{-N(H)Ph})(\mu_2\text{-H})(CO)_{10}$ gave $[Ru_3(\eta^2\text{-}\mu_3\text{-PhNCO})(\mu_2\text{-H})(CO)_{10}]^-$ with a bridging isocyanate ligand that was proposed to arise by addition of a μ_2-NPh ligand to a coordinated CO.[14] Addition of carbon monoxide to **23** concomitant with the cleavage of an Os–Os bond would give **12**, and displacement of one of the Os–N bonds in **12** by the addition of a second CO would yield **13**. Although intermediates **22** and **23** have not been detected, clusters **12** and **13** were spectroscopically characterized in this work. All steps up to the extrusion of PhN=C=O from the Os framework are likely to be reversible, and indeed it was shown that when **13a** was warmed under N_2, carbon monoxide was lost and cluster **7a** was re-formed. The final step is not reversible since the halide clusters $[Os_3X(CO)_{11}]^-$ do not react with PhN=C=O.

(22) Deeming, A. J.; Fuchita, Y.; Hardcastle, K.; Henrick, K.; McPartlin, M. *J. Chem. Soc., Dalton Trans.* **1986**, 2259.

An interesting observation is that the iodide-substituted imido clusters react more rapidly with CO than do the corresponding chloride clusters. This is exactly opposite the trend observed in the analogous Ru system where the chloride substituted imido cluster reacted more rapidly ($t_{1/2}$ = 8 min) with CO than did the iodide-substituted cluster ($t_{1/2}$ = 5 h).[2a] We rationalize these differing results by including in Scheme III the equilibrium between **7** and **8**, labeled K_{eq2}, along with a third equilibrium (K_{eq3}), which involves the concerted formation of the broken Os–Os bond and the displacement of one Os–imido bond. The values of K_{eq1} and K_{eq3} must be very small since only the imido halide clusters **7** and **8** were observed in solution under N_2 with no evidence seen for either **22** or **23**. Also, as shown above, K_{eq2} is much greater than 1 for the chloride cluster and is less than 1 for the iodide cluster. If we assume that K_{eq3} is very small, then **7** becomes a dead end with respect to the carbonylation of the imido ligand. This would explain the resistance to carbonylation exhibited by the chloride substituted cluster versus the relative ease of carbonylation exhibited by the iodide substituted cluster.

Finally, it should be noted that the η^2-μ_2-PhNCO clusters **13** are isoelectronic and isostructural with the η^2-μ_2-CH_2CO clusters previously described in these laboratories.[16] These compounds readily resulted from the carbonylation reaction 14. Like **13**, the ketene ligand in **24** undergoes al-

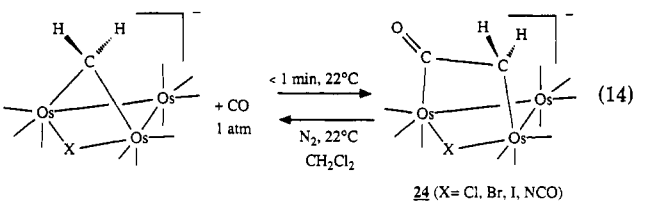

24 (X= Cl, Br, I, NCO)

kylation with methyl triflate and protonation to give methoxy- and hydroxy-σ,π-vinyl clusters, with the latter quickly rearranging to give an acyl ligand.[23] However, unlike **13**, the ketene clusters **24** do not undergo further carbonylation to release the ketene ligand.

Experimental Section

General Methods. The complex $Os_3(CO)_{12}$ was obtained from waste osmium solutions by the procedure reported by Keister,[24] and $Os_3(CO)_{11}(CH_3CN)$ was prepared according to the literature procedure.[25] Nitrosobenzene, 4-nitrotoluene, and [PPN]Cl were obtained from Aldrich Chemical Co. The salts [PPN]Br and [PPN]I were prepared from [PPN]Cl by metathesis according to literature methods[26] and were dried at 140 °C overnight. The reagent 4-nitrosotoluene was prepared from 4-nitrotoluene by appropriate modification of the published procedure for the synthesis of nitrosobenzene.[27] All solvents used were dried by distillation from CaH_2 (pentane, CH_2Cl_2, CH_3CN), Mg (MeOH), or sodium benzophenone ketyl (THF). All manipulations were performed under N_2 or Ar atmospheres in Schlenkware or in a Vacuum Atmospheres drybox, except for the chromatographic separations, which were performed in air. IR spectra were recorded on an IBM FT-IR/32 spectrometer operated in the absorbance mode, ^1H and ^{13}C NMR spectra were recorded on a Bruker AM-300 spectrometer, positive and negative ionization

(23) Bassner, S. L.; Geoffroy, G. L.; Rheingold, A. L. *Polyhedron* **1988**, *7*, 791.

(24) Keister, J. B. Ph.D. Thesis, The University of Illinois at Urbana-Champaign, 1978.

(25) (a) Johnson, B. F. G.; Lewis, J.; Pippard, D. A. *J. Chem. Soc., Dalton Trans.* **1981**, 407. (b) Nicholls, J. N.; Vargas, M. D. *Inorg. Synth.* **1989**, *26*, 289.

(26) Martinsen, A.; Songstad, J. *Acta Chem. Scand.* **1977**, *A31*, 645.

(27) (a) Vogel, A. I.; Furniss, B. S.; Hannaford, A. J.; Rogers, V.; Smith, P. W. G.; Tatchell, A. R. *Vogel's Textbook of Practical Organic Chemistry*, 4th ed.; Longman: New York, 1978; pp 723–724. (b) Robertson, P. S.; Vaughan, J. *J. Chem. Educ.* **1950**, *27*, 605.

fast atom bombardment (FAB) mass spectra were recorded on a Kratos MS50TC mass spectrometer, and electron impact (EI) mass spectra were recorded on a Kratos MS9/50 mass spectrometer. Elemental analyses were obtained from Galbraith Laboratories, Knoxville, TN.

Preparation of $Os_3(\mu_3\text{-}NPh)(CO)_{10}$. The cluster $Os_3(\mu_3\text{-}NPh)(CO)_{10}$ (**6**) was prepared by a modification of the literature procedure.[2b] The complex $Os_3(CH_3CN)(CO)_{11}$ (507 mg, 0.552 mmol) was dissolved in THF (200 mL), and a solution of PhNO (88.6 mg, 0.634 mmol) in THF (50 mL) was added dropwise over the course of 30 min. The solution was stirred for 30 min, the solvent was removed under vacuum, and the residue was chromatographed on a silica gel column with 1:9 CH_2Cl_2/hexane as eluent. The first band to elute was yellow $Os_3(CO)_{12}$ (98.5 mg, 20%). This was followed by a brown band of an unidentified compound (16.8 mg) [IR (hexane): ν_{CO} = 2102 (w), 2071 (vs), 2055 (m), 2035 (w), 2018 (vs), 2007 (s), 1996 (m), 1988 (m), 1979 (w) cm^{-1}]. The third band contained yellow $Os_3(\mu_3\text{-}NPh)(CO)_{10}$, which was isolated as a microcrystalline solid by solvent evaporation (280 mg, 54%) and was identified by its characteristic IR spectrum.[4] A fourth purple band containing a trace of an unidentified compound eluted next, and in some preparations a trace of a second purple compound would appear between the first and third bands. The cluster $Os_3(\mu_3\text{-}NTol)(CO)_{10}$ (**6′**) was isolated in 51% yield from an analogous reaction of $Os_3(CH_3CN)(CO)_{11}$ with 4-nitrosotoluene. ^{13}CO-enriched **6** (**6***) and **6′** (**6′***) were prepared as above using $Os_3(CO)_{12}$ that had been enriched to ~50% by the literature procedure.[13]

6. ^{13}C NMR (THF-d_8, −63 °C): δ 247.0 (s, 1 C, μ_3-*C*O), 176.2 (s, 3 C, Os-*C*O), 172.3 (s, 6 C, Os-*C*O), 165.2 (t, $^2J_{CH}$ = 7.0 Hz, NPh *ipso-C*), 131–123 (NPh *C*).

6′. Anal. Calcd for $C_{17}H_7NO_{10}Os_3$: C, 21.36; H, 0.74. Found: C, 21.53; H, 0.75. IR (pentane): ν_{CO} = 2103 (w), 2072 (vs), 2024 (vs), 2002 (w), 1692 (w) cm^{-1}. ^1H NMR (CD_2Cl_2): δ 7.2–6.9 (aryl), 2.30 (s, 3 H, Tol*CH*$_3$). ^{13}C NMR (THF-d_8, 23 °C): δ 244.1 (s, 1 C, μ_3-CO), 174.2 (s, 3 C, *axial* CO's), 170.8 (s, 6 C, *equatorial* CO's).

Reaction of $Os_3(\mu_3\text{-}NAr)(CO)_{10}$ with [PPN]Cl. To a THF solution (100 mL) of **6** (87.1 mg, 0.093 mmol) was added solid [PPN]Cl (53.0 mg, 0.092 mmol), and the solution was stirred for 2.5 h, during which time the yellow color darkened. The solvent was removed under vacuum, and the oily residue was washed twice with hexane. Six cycles of freezing pentane over the oily residue followed by quickly thawing under hot water and then removal of the pentane gave **7a** as an orange microcrystalline powder (93.5 mg, 68%). The analogous tolyl-substituted complex **7a′** was prepared as above using **6′** in place of **6**.

7a. Anal. Calcd for $C_{51}H_{35}ClN_2O_9Os_3P_2$: C, 41.17; H, 2.37. Found: C, 40.63; H, 2.38. IR (THF): ν_{CO} = 2072 (vw), 2033 (vs), 1988 (vs), 1954 (vs), 1914 (w), 1901 (w) cm^{-1}. ^{13}C NMR (THF-d_8, −68 °C): δ 194.4 (s, 2 C, Os-*C*O), 192.2 (s, 1 C, Os-*C*O), 185.2 (s, 2 C, Os-*C*O), 177.2 (s, 2 C, Os-*C*O), 176.5 (s, 2 C, Os-*C*O), 173.4 (t, $^2J_{CH}$ = 7.9 Hz, NPh *ipso-C*), 136–120 ([PPN]$^+$, NPh). MS (negative FAB, 18-crown-6/tetraglyme matrix): m/z = 950 (M^-, calcd m/z = 950).

7a′. Anal. Calcd for $C_{52}H_{37}ClN_2O_9Os_3P_2$: C, 41.59; H, 2.48. Found: C, 41.15; H, 3.01. IR (THF): ν_{CO} = 2050 (w), 2033 (s), 1988 (vs), 1960 (s), 1914 (w), 1901 (w) cm^{-1}. ^1H NMR (CD_2Cl_2): δ 7.5–7.2 ([PPN]$^+$), 7.11–6.86 (NPh), 2.23 (s, 3 H, Tol *CH*$_3$).

Reaction of $Os_3(\mu_3\text{-}NAr)(CO)_{10}$ with [PPN]I. To a THF solution (100 mL) of **6** (164 mg, 0.174 mmol) was added solid [PPN]I (133 mg, 0.200 mmol). The suspension was stirred for 4 h and filtered through Celite, and the solvent was removed under vacuum to leave a yellow-orange oily solid. Several cycles of freezing pentane over the oily residue followed by quickly thawing under hot water and then removal of the pentane left a microcrystalline yellow-orange powder (222 mg, 81%) containing mainly $[PPN][Os_3(\mu_3\text{-}NPh)(I)(CO)_9]$ (**8c**) but also a small amount of its isomer $[PPN][Os_3(\mu_3\text{-}NPh)(\mu_2\text{-}I)(CO)_9]$ (**7c**). An analogous reaction occurred with the tolyl-substituted compound **6′** to give **7c′** and **8c′**.

7c,8c Mixture. Anal. Calcd for $C_{51}H_{35}IN_2O_9Os_3P_2$: C, 38.79; H, 2.23. Found: C, 38.98; H, 2.44. IR (THF): ν_{CO} = 2070 (m), 2041 (vs), 2008 (vs), 1979 (vs), 1970 (s, sh), 1935 (m), 1657 (vw) cm^{-1}. ^{13}C NMR (THF-d_8, −73 °C): δ 234.4 (s, 1 C, μ_3-*C*O), 184.0 (s, 1 C, Os-*C*O), 181.8 (s, 1 C, Os-*C*O), 181.1 (s, 1 C, Os-*C*O), 179.8 (s, 1 C, Os-*C*O), 176.8 (s, 1 C, Os-*C*O), 176.5 (s, 1 C, Os-*C*O), 174.1 (s, 1 C, Os-*C*O), 173.9 (s, 1 C, Os-*C*O), 165.0 (br, 1 C, NPh *ipso-C*), 136–122 ([PPN]$^+$, NPh). MS (negative FAB, 18-crown-6/tetraglyme matrix): m/z = 1042 (M^-, calcd m/z = 1042).

7c′,8c′ Mixture. Anal. Calcd for $C_{52}H_{37}IN_2O_9Os_3P_2$: C, 39.20; H, 2.34. Found: C, 38.89; H, 2.21. IR (THF): ν_{CO} = 2083 (vw), 2070 (m), 2049 (sh, m), 2041 (2032, (sh, m), 2007 (s), 1993 (vs), 1984 (vs), 1971 (sh, m), 1935 (sh, w), 1914 (vw), 1901 (vw), 1659 (br, w) cm^{-1}. ^1H NMR (CD_2Cl_2) for **7c′**: δ 7.8–7.3 ([PPN]$^+$), 7.11–6.84 (NPh), 2.33 (s, 3 H Tol *CH*$_3$). ^1H NMR (CD_2Cl_2) for **8c′**: δ 7.8–7.3 ([PPN]$^+$), 7.06–6.86 (NPh), 2.25 (s, 3 H, Tol *CH*$_3$).

Reaction of $Os_3(\mu_3\text{-}NAr)(CO)_{10}$ with [PPN]Br. Cluster **6** (50.6 mg, 0.054 mmol) and [PPN]Br (33.2 mg, 0.054 mmol) were dissolved in THF (50 mL). After the sample was stirred for 3 h, IR analysis indicated the presence of **7b** and **8b** in a ~1:1 ratio. The mixture of these compounds was isolated as a yellow-orange microcrystalline solid by removal of the solvent under vacuum followed by freezing the resulting oily solid under pentane (61.2 mg, 0.040 mmol, 74%). The analogous tolyl-substituted imido cluster **6′** reacts in a similar manner to give a mixture of **7b′** and **8b′**.

7b,8b Mixture. Anal. Calcd for $C_{51}H_{35}BrN_2O_9Os_3P_2$: C, 39.98, H, 2.30. Found: C, 39.71, H, 2.50. IR (THF): ν_{CO} = 2072 (w), 2042 (s), 2033 (m), 2010 (m), 1989 (vs), 1980 (s, sh), 1968 (s), 1963 (m), 1956 (m), 1910 (vw, **7b**), 1900 (vw, **7b**), 1665 (vw, μ_3-CO of **8b**) cm^{-1}.

7b′,8b′ Mixture. IR (THF): ν_{CO} = 2084 (sh, w), 2072 (m), 2041 (s), 2033 (s), 2010 (s), 1988 (vs), 1958 (m), 1932 (sh, w), 1913 (w), 1902 (w), 1671 (vw) cm^{-1}. ^1H NMR (CD_2Cl_2) for **7b′**: δ 7.33–6.86 (NTol aryl), 2.31 (s, 3 H, Tol *CH*$_3$). ^1H NMR (CD_2Cl_2) for **8b′**: δ 7.14–6.88 (NTol aryl), 2.22 (s, 3 H, Tol *CH*$_3$).

Protonation of $[PPN][Os_3(\mu_3\text{-}NPh)(\mu_2\text{-}Cl)(CO)_9]$ (7a). Compound **7a** was generated in situ by combining the imido cluster **6** (22.7 mg, 0.0241 mmol) with [PPN]Cl (18.8, 0.0327 mmol) in THF (25 mL). The solution was filtered through Celite and then chilled to −80 °C. Carbon monoxide was bubbled vigorously through the solution for 15 min, the flask was sealed under 1 atm of CO, CF_3CO_2H (4 μL, 0.05 mmol) was added, and the solution was allowed to warm to room temperature, during which time the color changed from yellow-brown to a slightly greenish yellow. The solvent was removed under vacuum, and the residue was chromatographed on silica gel TLC plates using 1:9 CH_2Cl_2/hexane as eluent. Although five bands were apparent, only the third band gave sufficient product to isolate. The other trace bands were identified by their color and retention factors. The first band was red $Os_3(\mu_2\text{-}Cl)(\mu_2\text{-}H)(CO)_{10}$, and the second band was yellow $Os_3(exo\text{-}\mu_2\text{-}N(H)Ph)(\mu_2\text{-}Cl)(CO)_{10}$ (**10a**). The third band proved to be **9a** (21.1 mg, 84%), which was isolated as a pale yellow powder. The fourth band was yellow $Os_3(endo\text{-}\mu_2\text{-}N(H)Ph)(\mu_2\text{-}Cl)(CO)_{10}$ (**11a**), but the fifth band was not identified. From an analogous protonation using $HBF_4{\cdot}Et_2O$, compounds **10a** and **11a** were isolated in higher but variable yields, and their spectroscopic data are summarized below.

9a. Anal. Calcd for $C_{15}H_6ClNO_9Os_3$: C, 18.96; H, 0.64. Found: C, 19.02; H, 0.63. IR (pentane): ν_{CO} = 2117 (w), 2083 (m), 2054 (vs), 2043 (w), 2029 (m), 2007 (s), 1993 (m), 1975 (w) cm^{-1}. ^1H NMR (THF-d_8): δ 7.52–6.98 (m, 5 H, aryl), −12.19 (s, 1 H, Os-*H*-Os). ^{13}C NMR (THF-d_8, 1 mg of Cr(acac)$_3$, −73 °C): δ 187.0 (s, 1 C, Os-*C*O), 182.1 (s, 1 C, Os-*C*O), 176.4 (s, 1 C, Os-*C*O), 176.1 (d, $^2J_{CH}$ = 11.4 Hz, 1 C, H-Os-*C*O), 173.8 (s, 1 C, Os-*C*O), 173.4 (s, 1 C, Os-*C*O), 172.9 (br, 1 C, Os-*C*O), 169.3 (br t, 1 C, NPh *ipso-C*), 167.6 (d, $^2J_{CH}$ = 17.7 Hz, 1 C, H-Os-*C*O), 164.4 (s, 1 C, Os-*C*O), 132–127 (aryl). MS (FAB, 18-crown-6/tetraglyme matrix): m/z = 951 (M^+, calcd m/z = 951).

10a. Anal. Calcd for $C_{16}H_6ClNO_{10}Os_3$: C, 19.64; H, 0.62. Found: C, 19.94; H, 0.74. IR (pentane): ν_{CO} = 2106 (w), 2074 (s), 2058 (m), 2036 (vw), 2021 (s), 2005 (vs), 1985 (w), 1973 (vw) cm^{-1}. ^1H NMR (CD_2Cl_2): δ 7.31–7.02 (aryl), 3.64 (br, 1 H, PhN*H*). ^{13}C NMR (THF-d_8, −73 °C): δ 185.1 (s, 1 C, Os-*C*O), 180.0 (s, 2 C, Os-*C*O), 179.5 (s, 1 C, Os-*C*O), 177.1 (s, 2 C, Os-*C*O), 177.0 (s, 2 C, Os-*C*O), 167.7 (s, 2 C, Os-*C*O), 166.8 (t, $^3J_{CH}$ = 6.4 Hz, 1 C, Ph *ipso-C*), 131–118 (aryl). MS (EI): m/z = 979 (M^+, calcd m/z = 979).

11a. IR (pentane): ν_{CO} = 2106 (vw), 2071 (vs), 2057 (m), 2019 (vs), 1996 (s), 1985 (m) cm^{-1}. ^1H NMR (CD_2Cl_2): 7.4–7.0 (aryl), 5.17 (br, 1 H, *H*NPh). ^{13}C NMR (THF-d_8, −73 °C): δ 183.2 (s, 2 C, Os-*C*O), 181.2 (s, 1 C, Os-*C*O), 180.2 and 180.1 (two over-

lapping peaks which could not be separately integrated, 3 C, Os–*C*O), 179.8 (s, 2 C, Os–*C*O), 168.2 (s, 2 C, Os–*C*O), 153.2 (m, 1 C, NPh *ipso-C*), 131–125 (aryl). MS (EI): m/z = 979 (M^+, calcd m/z = 979).

Protonation of [PPN][$Os_3(\mu_3$-NPh)(I)$(CO)_9$] (8c). Complex **8c** was generated in situ from cluster **6** (103 mg, 0.11 mmol) and [PPN]I (84 mg, 0.13 mmol) in THF (50 mL), and CF_3CO_2H (1 mL, 13.0 mmol) was added. The solution was stirred overnight, and the solvent was removed under vacuum. The residue was chromatographed on silica gel TLC plates with 1:9 CH_2Cl_2/hexane to give four yellow bands. The first two bands were traces of $Os_3(CO)_{12}$ and yellow $Os_3(exo$-μ_2-N(H)Ph)(μ_2-I)$(CO)_{10}$ (**10c**). The third band was pale yellow $Os_3(\mu_3$-NPh)(μ_2-H)(μ_2-I)$(CO)_9$ (**9c**) (36.6 mg, 32%), which was recrystallized from pentane. The last band was yellow $Os_3(endo$-μ_2-N(H)Ph)(μ_2-I)$(CO)_{10}$ (**11c**) (8.0 mg, 0.008 mmol, 7%). Similar results were obtained when the protonation was performed under 1 atm of CO except that the first band was red $Os_3(\mu_2$-H)(μ_2-I)$(CO)_{10}$ (1.1 mg, 2%). The second band was **10c** (4.8 mg, 8%), the third was **9c** (12.8 mg, 22%), and the fourth band was in the tail of **9c** and consisted of <1 mg of **11c**.

9c. Anal. Calcd for $C_{15}H_6INO_9Os_3$: C, 17.30; H, 0.58. Found: C, 17.23; H, 0.59. IR (pentane): ν_{CO} = 2114 (w), 2080 (s), 2052 (vs), 2040 (w), 2027 (m), 2007 (vs), 1991 (m), 1973 (w) cm^{-1}. ^1H NMR (CD_2Cl_2): δ 7.41–6.99 (aryl), –13.34 (s, 1 H, Os–*H*–Os). MS (EI): m/z = 1042 (M^+ – H, calcd m/z = 1043).

10c. IR (pentane) ν_{CO} = 2105 (w), 2072 (s), 2057 (m), 2019 (m), 2007 (vs), 1993 (w), 1984 (w), 1973 (vw) cm^{-1}. ^1H NMR (CD_2Cl_2): δ 7.31–6.97 (aryl), 3.88 (br, 1 H, PhN*H*). MS (EI): m/z = 1070 (M^+ – H, calcd m/z = 1071).

11c. IR (pentane) ν_{CO} = 2105 (w), 2067 (s), 2053 (m), 2018 (vs), 2005 (m), 1995 (m), 1981 (w). ^1H NMR (CD_2Cl_2): δ 7.3–7.1 (m, 5 H, aryl), 4.73 (br, 1 H, PhN*H*). MS (EI): m/z = 1071 (M^+, calcd m/z = 1071).

Carbonylation of 7a. Complex **7a** was generated as described above from cluster **6** (53.8 mg, 0.057 mmol) and [PPN]Cl (40.3 mg, 0.070 mmol) in THF (50 mL). Carbon monoxide was vigorously bubbled through the solution for 15 min, the flask was sealed under 1 atm of CO, and the solution was stirred for 93 h. After this time the IR data indicated the presence of [PPN]-[$Os_3(\eta^2$-μ_2-PhNCO)(μ_2-Cl)$(CO)_{10}$] (**13a**) and [PPN][Os_3(Cl)$(CO)_{11}$] (**14a**), but due to heavily overlapping bands it was not possible to estimate the relative concentrations of each species. Evaporation of the solvent under vacuum left an orange-yellow microcrystalline solid which consisted of a mixture of **13a** and **14a**. The ^{13}CO-enriched tolyl-substituted analogue **13a'*** was prepared in higher purity by adding a concentrated CH_2Cl_2 solution of [PPN]Cl to a concentrated THF solution of **6'***, followed by stirring for 0.5 h and then stirring under ^{13}CO (99% ^{13}C, Isotech) for 71 h.

13a,14a Mixture. IR (THF): ν_{CO} = 2087 (w), 2052 (s), 2033 (m), 2000 (sh, m), 1993 (vs), 1967 (m), 1950 (sh, w), 1912 (w) cm^{-1}. MS (FAB, 18-crown-6/tetraglyme matrix): m/z = 1006 (M^-, calcd m/z = 1006 for **13a**).

13a. ^{13}C NMR (THF-d_8, –73 °C): δ 198.9 (s, PhN*C*O), 189–168 (Os–*C*O).

13a'*. ^1H NMR (THF-d_8, –63 °C): δ 7.0–6.8 (m, 4 H, Tol *H*'s), 2.18 (s, 3 H, Tol C*H*$_3$). ^{13}C NMR (THF-d_8, –63 °C): δ 198.1 (d, $^2J_{CC}$ = 29.0 Hz, 1 C, TolN*C*(O)–Os–CO), 187.9 (d, $^2J_{CC}$ = 29.3 Hz, 1 C, TolNC(O)–Os–*C*O), 187.2 (d, $^2J_{CC}$ = 32.4 Hz, 1 C, OC–Os–*C*O), 185.5 (s, 1 C, Os–*C*O), 183.4 (d, $^2J_{CC}$ = 33.4 Hz, 1 C, OC–Os–*C*O), 182.4 (s, 2 C, Os–*C*O), 182.0 (s, 1 C, Os–*C*O), 180.9 (s, 1 C, Os–*C*O), 171.8 (s, 1 C, Os–*C*O), 169.2 (s, 1 C, Os–*C*O).

Carbonylation of 8c. Complex **8c** was generated as described above from cluster **6** (103.2 mg, 0.110 mmol) and [PPN]I (89.5 mg, 0.135 mmol) in THF (100 mL). Carbon monoxide was vigorously bubbled through the solution for 15 min, the flask was sealed under 1 atm of CO, and the solution was stirred for 14 h. After this time the IR spectrum of the solution indicated the presence of [PPN][$Os_3(\eta^2$-μ_2-PhNCO)(μ_2-I)$(CO)_{10}$] (**13c**) and [PPN][Os_3I$(CO)_{11}$] (**14c**). Heavily overlapping bands precluded an accurate estimation of the relative amounts of each species. Removal of the solvent under vacuum left an orange-yellow microcrystalline powder. Shorter carbonylation times (5 h) of the tolyl-substituted derivative **6'** led to mixtures of [PPN]-[$Os_3(\eta^2$-μ_3-TolNCO)(μ_2-I)$(CO)_9$], **12c'**, and **13c'**. The tolyl-substituted analogues **13c'** and **13c'*** were prepared in higher purity by adding a concentrated CH_2Cl_2 solution of [PPN]I to a concentrated THF solution of **6'** or **6'*** followed by stirring for 0.5 h and then stirring under CO or ^{13}CO (99% ^{13}C, Isotech) for 14 h. Higher purity **12c** and **12c'** were prepared by adding a concentrated CH_2Cl_2 solution of [PPN]I to a concentrated THF solution of **6** or **6'**, stirring for 0.5 h, and then stirring under 1 atm of CO for 5 h each.

13c,14c Mixture. IR (THF): ν_{CO} = 2083 (w), 2063 (sh, w), 2047 (s), 2032 (m), 1993 (vs), 1970 (m), 1954 (w) cm^{-1}. MS (FAB, 18-crown-6/tetraglyme matrix): m/z = 1098.2 (M^-, calcd = m/z = 1098).

12c. ^{13}C NMR (CD_2Cl_2, –63 °C): δ 193.7 (s, 1 C, PhN*C*O), 185.7 (s, 1 C, Os–*C*O), 181.8 (s, 1 C, Os–*C*O), 181.6 (s, 1 C, Os–*C*O), 179.0 (s, 2 C, Os–*C*O), 178.3 (s, 1 C, Os–*C*O), 177.1 (s, 1 C, Os–*C*O), 168.4 (s, 1 C, Os–*C*O), 166.4 (s, 1 C, Os–*C*O), 157.5 (br, 1 C, PhN *ipso-C*), 130–120 (m, PhN *C*'s).

12c'. ^1H NMR (CD_2Cl_2): δ 7.2–6.8 (m, 4 H, NTol aryl), 2.34 (s, 3 H, NTol C*H*$_3$). ^{13}C NMR (CD_2Cl_2, –63 °C): δ 193.8 (s, 1 C, TolN*C*O), 185.8 (s, 1 C, Os–*C*O), 182.0 (s, 1 C, Os–*C*O), 181.8 (s, 1 C, Os–*C*O), 179.2 (s, 1 C, Os–*C*O), 179.1 (s, 1 C, Os–*C*O), 177.5 (s, 1 C, Os–*C*O), 177.3 (s, 1 C, Os–*C*O), 168.5 (s, 1 C, Os–*C*O), 166.5 (s, 1 C, Os–*C*O), 160.6 (br, 1 C, TolN *ipso-C*).

12c'*. ^1H NMR (THF-d_8, –73 °C): δ 6.91 (d, 2 H, tolyl), 6.76 (d, 2 H, tolyl), 2.15 (s, 3 H, Tol C*H*$_3$). ^{13}C NMR (THF-d_8, –73 °C): δ 192.3 (d, $^2J_{CC}$ = 29.0 Hz), 189–170 (Os–CO).

13c. ^{13}C NMR (THF-d_8, –73 °C): δ 198.3 (s, PhN*C*O), 188–166 (Os–*C*O).

13c'*. ^{13}C NMR (CD_2Cl_2, 23 °C): δ 197.4 (d, $^2J_{CC}$ = 29 Hz, PhN*C*(O)), 185.8 (d, $^2J_{CC}$ = 35 Hz, Os–CO), 183.6 (d, $^2J_{CC}$ = 33 Hz, Os–CO), 182.5 (d, $^2J_{CC}$ = 31 Hz, Os–*C*O), 183–166 (Os–*C*O).

13c'*. ^1H NMR (THF-d_8, –73 °C): δ 7.1–6.4 (m, 4 H, TolN aryl), 2.30 (s, 3 H, Tol C*H*$_3$). ^{13}C NMR (CD_2Cl_2): δ 197.5 (d, $^2J_{CC}$ = 29 Hz, PhN*C*(O)), 188.2 (d, $^2J_{CC}$ = 32 Hz, Os–*C*O), 185.9 (d, $^2J_{CC}$ = 33 Hz, Os–*C*O), 183.8 (d, $^2J_{CC}$ = 29 Hz, Os–*C*O), 183–165 (Os–CO's).

Alkylation of 13a with $CF_3SO_3CH_3$. Cluster **13a** was generated in situ from complex **6** (53.8 mg, 0.059 mmol) and [PPN]Cl (40.3 mg, 0.070 mmol) of THF (50 mL) as described above. The THF was removed under vacuum, the residue was dissolved in CH_2Cl_2 (50 mL), the solution was chilled to –80 °C, and CO bubbled vigorously through the solution for 15 min. Then $CF_3SO_3CH_3$ (10 μL, 0.088 mmol) was added, and the solution was allowed to warm to room temperature. The solvent was removed under vacuum, and the residue was chromatographed on silica gel TLC plates using 1:9 CH_2Cl_2/hexane as eluent. The first band to elute was a trace of yellow $Os_3(CO)_{12}$, the second was yellow **10a** (2.5 mg, 4%), the third was pale yellow $Os_3(\mu_2$-PhNCOCH$_3$)(μ_2-Cl)$(CO)_{10}$ (**17a**) (13.3 mg, 22%), and the fourth band was 1.0 mg of an unidentified yellow compound. Two additional low-yield bands (3.2 mg) with low R_f values were observed but were not identified.

17a. Anal. Calcd for $C_{18}H_8ClNO_{11}Os_3$: C, 21.19; H, 0.79. Found: C, 21.53; H, 0.75. IR (pentane): ν_{CO} = 2105 (w), 2074 (vs), 2053 (m), 2035 (vw), 2021 (s), 2007 (vs), 1993 (m), 1984 (w), 1974 (w), 1954 (vw) cm^{-1}. ^1H NMR (CD_2Cl_2, 22 °C): δ 7.44 (t, 2 H, NPh *m*-H), 7.19 (t, 1 H, NPh *p*-H), 7.08 (br, 2 H, NPh *o*-H), 3.97 (s, 3 H, PhNCOC*H*$_3$).

Alkylation of 13c with $CF_3SO_3CH_3$. The cluster **13c** was generated in situ from complex **6** (103.2 mg, 0.114 mmol) and [PPN]I (89.5 mg, 0.135 mmol) in THF (100 mL) as described above. The THF was removed under vacuum, and the residue was dissolved in CH_2Cl_2 (100 mL) to give a brownish-yellow solution, which was chilled to –80 °C. Carbon monoxide was bubbled through the solution for 15 min, $CF_3SO_3CH_3$ (15 μL, 0.13 mmol) was added, and the solution was allowed to warm to room temperature without appreciable color change. The solvent was removed under vacuum and the residue chromatographed on silica gel plates using 1:9 CH_2Cl_2/hexane as eluent. The first band to elute was yellow **10c** (2.3 mg, 2%), the second was pale yellow $Os_3(\mu_2$-PhNCOCH$_3$)(μ_2-I)$(CO)_{10}$ (**17c**) (54.5 mg, 43%), and the third band contained a trace of a yellow unidentified complex.

17c. Anal. Calcd for $C_{18}H_8INO_{11}Os_3$: C, 19.45; H, 0.73. Found: C, 19.67; H, 0.87. IR (pentane): ν_{CO} = 2102 (w), 2069 (vs), 2052 (m), 2019 (s), 2007 (vs), 2001 (s), 1993 (m), 1982 (w), 1973 (w) cm^{-1}. ^1H NMR (CD_2Cl_2, 22 °C): δ 7.41 (t, 2 H, NPh *m*-H), 7.15 (t, 1 H, NPh *p*-H), 6.92 (br dd, 2 H, NPh *o*-H), 3.88 (s, 3 H,

PhNCOCH_3). ^{13}C NMR (THF-d_8, −73 °C, 1 mg of Cr(acac)$_3$): δ 205.1 (br, 1 C, PhNCOCH$_3$), 185.8 (s, 1 C, Os–CO), 185.4 (s, 1 C, Os–CO), 181.9 (s, 1 C, Os–CO), 181.4 (s, 1 C, Os–CO), 178.7 (s, 1 C, Os–CO), 178.6 (s, 1 C, Os–CO), 176.8 (s, 1 C, Os–CO), 176.2 (s, 1 C, Os–CO), 167.4 (s, 1 C, Os–CO), 166.6 (s, 1 C, Os–CO), 156.7 (br t, 1 C, PhNCOCH$_3$ *ipso*-C), 131.3–127.7 (aryl carbons), 62.1 (q, $^1J_{CH}$ = 147 Hz, PhNCOCH$_3$).

Protonation of 13a. Cluster **13a** was generated in situ from cluster **6** (256 mg, 0.272 mmol) and [PPN]Cl (170 mg, 0.295 mmol) in THF (150 mL) as described above. The solution was chilled to −80 °C, carbon monoxide was bubbled vigorously through the solution for 15 min, CF_3CO_2H (25 μL, 0.32 mmol) was added, the solution was allowed to warm to room temperature, and the solvent was removed under vacuum. The yellow/brown residue was chromatographed on silica gel plates using 2:3 CH_2Cl_2/hexane as eluent. Five bands were observed, but the third purple band was not isolated because of its low yield. The first band was yellow $Os_3(exo\text{-}\mu_2\text{-}N(H)Ph)(\mu_2\text{-}Cl)(CO)_{10}$ (**10a**) (9.3 mg, 4%), the second was pale yellow $Os_3(\mu_3\text{-}NPh)(\mu_2\text{-}Cl)(\mu_2\text{-}H)(CO)_9$ (**9a**) (6.9 mg, 3%), the fourth was yellow $Os_3(endo\text{-}\mu_2\text{-}N(H)Ph)(\mu_2\text{-}C)(CO)_{10}$ (**11a**) (2.3 mg, 1%), and the fifth was pale yellow $Os_3(\mu_2\text{-}PhNCOH)(\mu_2\text{-}Cl)(CO)_{10}$ (**19a**) (64.4 mg, 24%). The use of $HBF_4{\cdot}Et_2O$ in the protonation reactions gave higher yields of **10a** and **11a** at the expense of **19a**, but the yields were variable.

19a. Anal. Calcd for $C_{17}H_6ClNO_{11}Os_3$: C, 20.29; H, 0.60. Found: C, 21.40; H, 1.02. IR (pentane): ν_{CO} = 2107 (w), 2075 (vs), 2055 (m), 2023 (vs), 2005 (vs), 2000 (vs), 1980 (w), 1596 (vw), 1507 (w) cm^{-1}. ^{1}H NMR (CD_2Cl_2, 22 °C): δ 7.78 (s, 1 H, PhNCO*H*), 7.58 (t, 2 H, Ph *m*-H), 7.40 (t, 1 H, Ph *p*-H), 7.19 (d, 2 H, Ph *o*-H). ^{13}C NMR (THF-d_8, 1 mg of Cr(acac)$_3$, −73 °C): δ 203.6 (s, 1 C, PhNCOH), 187.1 (s, 1 C, Os–CO), 185.8 (s, 1 C, Os–CO), 184.7 (s, 1 C, Os–CO), 183.3 (s, 1 C, Os–CO), 180.4 (s, 1 C, Os–CO), 179.6 (s, 1 C, Os–CO), 179.4 (s, 1 C, Os–CO), 178.5 (s, 1 C, Os–CO), 168.9 (s, 1 C, Os–CO), 168.4 (s, 1 C, Os–CO), 154.9 (br, 1 C, Ph *ipso*-C), 132–122 (Ph carbons). MS (EI): m/z = 1007 (M^+, calcd m/z = 1007).

Protonation of 13c. Complex **13c** was generated in situ from cluster **6** (40.8 mg, 0.043 mmol) and [PPN]I (33.3 mg, 0.050 mmol) in THF (50 mL) as described above. The solution was chilled to −80 °C, CF_3CO_2H (5 μL, 0.065 mmol) was added under 1 atm of CO, and the solution was allowed to warm to room temperature. The solvent was removed under vacuum, and the residue was chromatographed on silica gel TLC plates using 3:7 CH_2Cl_2/hexane as the eluent. Four bands were isolated. The first was yellow $Os_3(endo\text{-}\mu_2\text{-}N(H)Ph)(\mu_2\text{-}I)(CO)_{10}$ (**10c**) (2.1 mg, 5%), the third was pale yellow $Os_3(\mu_3\text{-}NPh)(\mu_2\text{-}H)(\mu_2\text{-}I)(CO)_9$ (**9c**) (2.1 mg, 5%), the fourth was yellow $Os_3(endo\text{-}\mu_2\text{-}N(H)Ph)(\mu_2\text{-}I)(CO)_{10}$ (**11c**) (1.4 mg, 3%), the fifth was 1.1 mg of an unidentified compound, and the sixth band was pale yellow $Os_3(\mu_2\text{-}PhNCOH)(\mu_2\text{-}I)(CO)_{10}$ (**19c**) (24.0 mg, 51%).

19c. IR (CH_2Cl_2) ν_{CO} = 2100 (w), 2069 (vs), 2050 (m), 2015 (vs), 2004 (s), 1974 (m, sh), 1943 (vw, sh) cm^{-1}. ^{1}H NMR (CD_2Cl_2, 23 °C): δ 9.61 (br, 1 H, PhNCO*H*), 7.47 (t, 2 H, Ph *m*-*H*), 7.25 (t, 1 H, Ph *p*-*H*), 7.02 (d, 2 H, Ph *o*-*H*). ^{13}C NMR (DMSO-d_6, 22 °C): δ 196.0 (s, PhNCOH), 184.4 (s, 1 C, Os–CO), 183.6 (s, 1 C, Os–CO), 181.5 (s, 1 C, Os–CO), 180.2 (s, 1 C, Os–CO), 177.9 (s, 1 C, Os–CO), 176.3 (s, 1 C, Os–CO), 176.1 (s, 1 C, Os–CO), 175.1 (s, 1 C, Os–CO), 165.6 (s, 1 C, Os–CO), 165.3 (s, 1 C, Os–CO). Anal. Calcd for $C_{16}H_6INO_{10}Os_3$: C, 17.97; H, 0.57. Found: C, 20.85; H, 0.89. Several attempts to obtain an acceptable analysis on this otherwise well-characterized compound failed. The tolyl-substituted analogue **19c′**, which was prepared in a similar manner and gave similar spectroscopic data, gave an acceptable analysis. Anal. Calcd for $C_{18}H_8INO_{11}Os_3$ (**19c′**): C, 19.45; H, 0.73. Found: C, 19.83; H, 0.78.

Crystal Structure Determination of [PPN][$Os_3(\mu_3\text{-}NPh)(\mu_2\text{-}C)(CO)_9$] (7a), $Os_3(\mu_2\text{-}exo\text{-}N(H)Ph)(\mu_2\text{-}Cl)(CO)_{10}$ (10a), $Os_3(endo\text{-}\mu_2\text{-}N(H)Ph)(\mu_2\text{-}Cl)(CO)_{10}$ (11a), and $Os_3(\eta^2\text{-}\mu_2\text{-}PhNCOCH_3)(\mu_2\text{-}I)(CO)_{10}$ (17c). Crystal, data collection, and refinement parameters are collected in Table I. Well-formed crystals of **7a**, **10a**, **11a**, and **17c** were each mounted on fine glass fibers with epoxy cement, and the unit cell parameters of each were determined from the least squares fit of 25 reflections ($20° \le 2\theta \le 25°$). Preliminary photographic characterizations showed $2_1/m$ Laue symmetry for **7a**, **10a**, and **17c** and *mmm* Laue symmetry for **11a**. The systematic absences in the diffraction data of **7a** uniquely established the space group as $P2_1/c$. The systematic absences in the diffraction data of **10a** and **17c** established that the group was either *Cc* or *C*2/*c*. The *E*-statistics for both **10a** and **17c** suggested the centrosymmetric alternative and the chemically sensible results of refinement indicated that the assignment was correct. The systematic absences in the diffraction data of **11a** uniquely established the space group as *Pccn*. An empirical absorption correction was applied to each of the data sets (216 ψ-scan reflections; pseudoellipsoid model). The semiempirical absorption correction program XABS was applied to the data of **10a**, **11a**, and **17c**.

The structures were each solved by direct methods, which located the Os atoms. The remaining non-hydrogen atoms were located through subsequent difference Fourier and least squares syntheses. All hydrogen atoms were included as idealized isotropic contributions (d(CH) = 0.960 Å, $U = 1.2U$ for attached C). All non-hydrogen atoms were refined with anisotropic thermal parameters. Phenyl rings were fixed as rigid planar hexagons (d(CC) = 1.395 Å). In **10a** (Figure 3) the bond between the nitrogen atom and the *ipso*-carbon of the phenyl ring is approximately perpendicular to the Os(1)–Os(2)–Os(3) plane, and in **11a** (Figure 4) the same bond is nearly parallel to the triosmium plane. The unit cell of **17c** contains several grouped atoms remote from the Os_3 clusters labeled CS(1) to CS(6) for which no positive chemical identification could be made. These atoms were treated as carbon atoms of unknow, disordered solvent molecules.

All computer programs and the sources of the scattering factors are contained in the SHELXTL program library (version 5.1) (Sheldrick, G. Nicolet (Siemens), Madison, WI).

Acknowledgment. We gratefully acknowledge the Department of Energy, Office of Basic Energy Sciences, and ARCO Chemical Co. for funding this research as well as the National Science Foundation for partially funding the purchase of the diffractometer at the University of Delaware.

Supplementary Material Available: Table A, listing NMR data for Os_3 compounds, and, for **7a**, **10a**, **11a**, and **17c**, complete lists of bond lengths and angles, anisotropic thermal parameters, calculated hydrogen atom positions, and isotropic thermal parameters (14 pages); tables of observed and calculated structure factors (39 pages). Ordering information is given on any current masthead page.